APRIL 2026

SEISMIC ACADEMY

Trimester publication

EPICENTRE

Special Issue VOL 11
Long Bridge with Tall Piers under Seismic Excitation

Seismic Splendour
Atmosphere Sky Bridge (Deya)

Interactive Crossword

SEISMIC ACADEMY

A forum for **professionals**, **academicians**, **authorities** and **industry experts** to interact and disseminate knowledge on various aspects of **earthquake engineering with different stakeholders**, with an intent to **increase awareness** and develop their expertise on the subject.

Our Vision

To make the seismic academy a one-stop source of information and use it for the promotion of all seismic initiatives in our country.

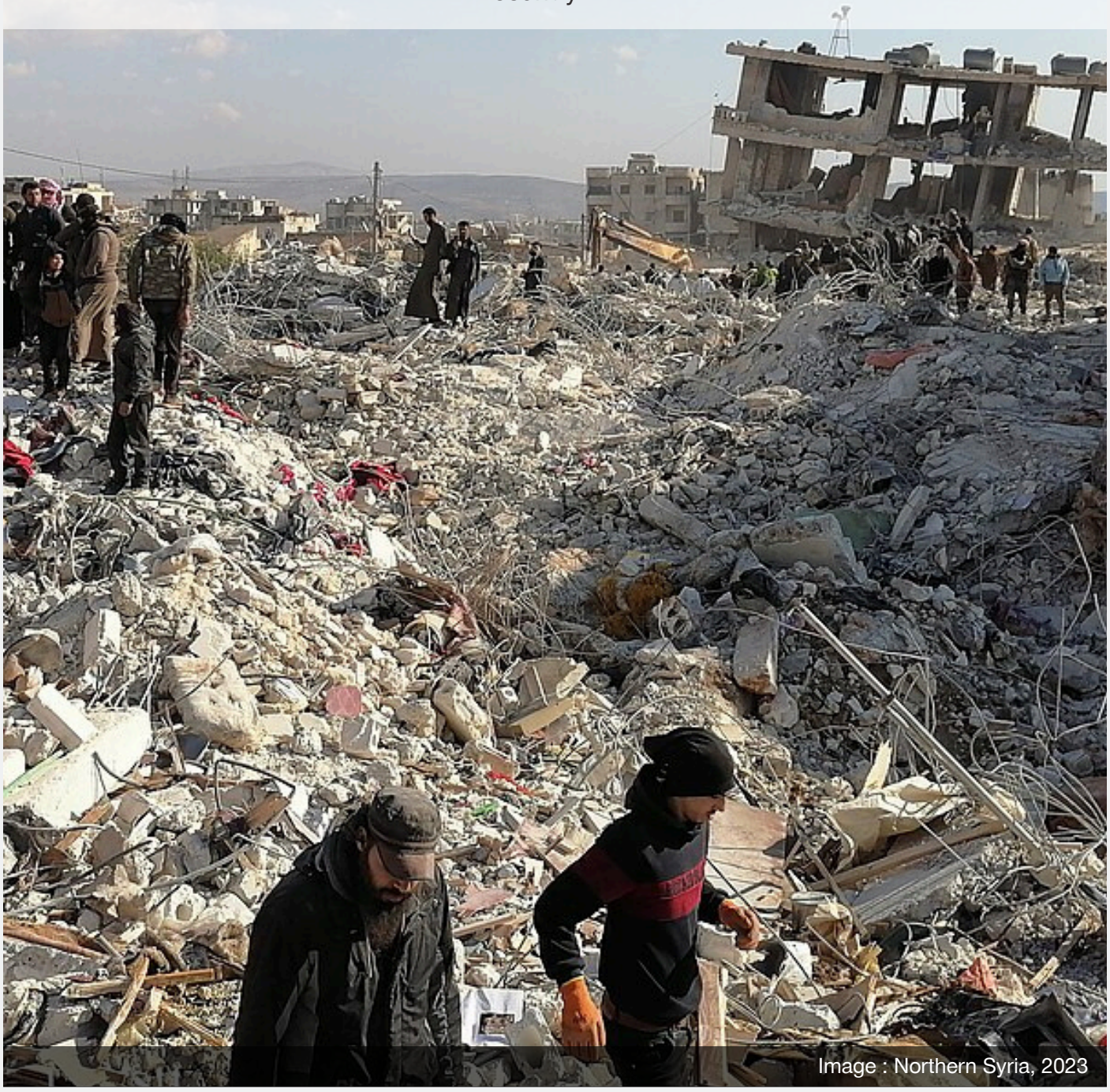

Image : Northern Syria, 2023

Our Advisory Board

Er. Jayant Kumar
Managing Director
Hilti India Pvt. Ltd.

Dr. Rajeev Goel
Chief Scientist & Head
Bridge Engg. & Struct. Div.
CSIR-CBRI, New Delhi

Dr. S M Ali
Director General
Solar Energy Society
of India

Dr. Durgesh Rai
Professor, Dept. of Civil
Engineering
IIT - Kanpur

Er. Vinay Gupta
Managing Director
M/S Tandon
Consultants Pvt. Ltd.

Er. Sangeeta Wij
Managing Partner
SD Engineering Consultants

Er. Alok Bhowmick
Managing Director
B&S Engineering
Consultants Pvt. Ltd.

Dr. Vasant Matsagar
Dogra Chair Prof.
Dept. of Civil Engg.
IIT Delhi

Dr. Amit Prashant
Professor of Civil Engg.
and Dean of Research &
Devt. IIT Gandhinagar

Er. Gangeshwar Kawale
Member, MEP Engineers
Association

Dr. Ajay Chourasia
Chief Scientist and Head
of Structural Engg. & 3D
Concrete Printing Group
CSIR-CBRI, Roorkee

Dr. Harshavardhan Subbarao
Chairman & Managing
Director, Construma
Consultancy Pvt. Ltd.

For further information, contact -
Agamoni Das, Head - Codes & Approvals (Fastening), Hilti India Pvt. Ltd.
M: 8826565647 | E: support@theseismicacademy.com

An initiative by HILTI
Building Benchmarks for Industry and Academia

An ethos EMPOWERS www.ethosempowers.com **Production**

Table of Contents

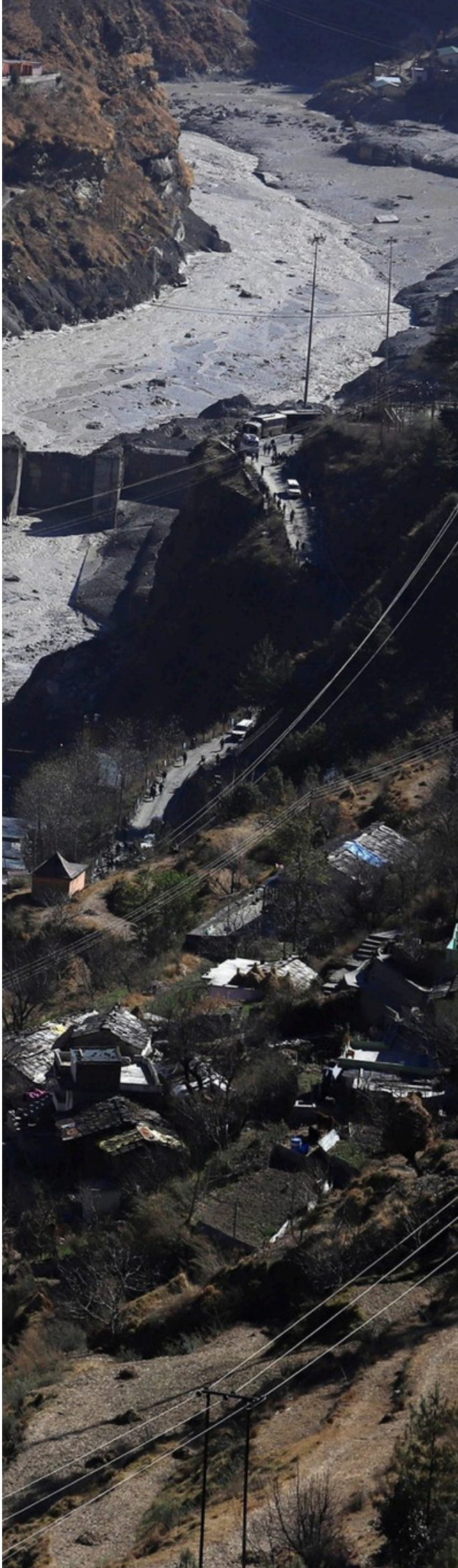

> **A safer India is built not only on stronger structures, but on smarter predictions; Probabilistic Seismic Hazard Assessment brings science and foresight together to redefine seismic safety.**

2015, the Gorkha earthquake in Nepal

Webinar

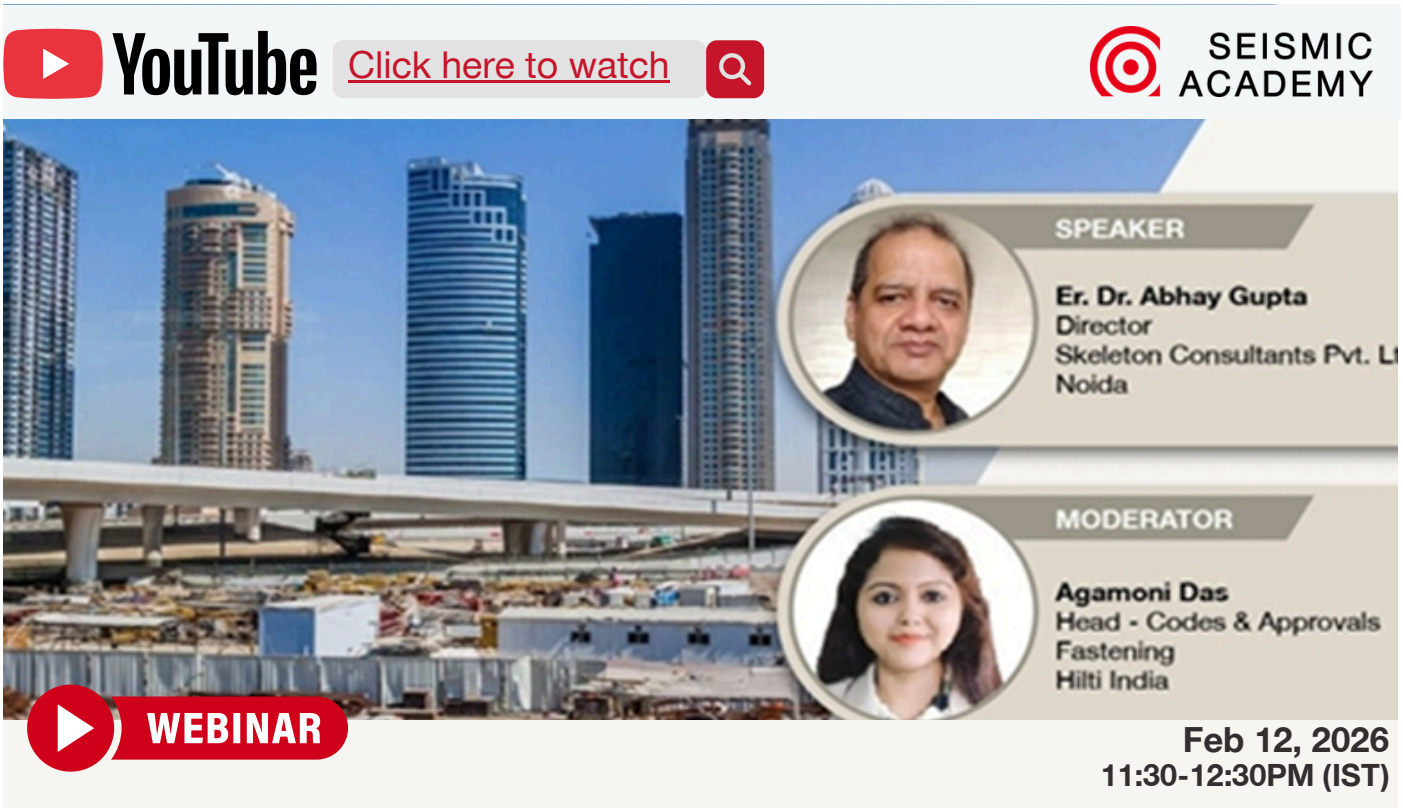

Seismic Design of Steel Structures: From Theory to Practice

Seismic academy organized a technical webinar on “Seismic Design of Steel Structures” with the objective of strengthening industry understanding of earthquake-resistant design principles and their practical application in steel construction in the month of February 2026.
The session was delivered by **Er. Dr. Abhay Gupta**, Director, Skeleton Consultants Pvt. Ltd and was moderated by **Er. Agamoni Das**, Head-Codes & Approvals (Fastening), Hilti India.

The session began with the context highlighting the growing relevance of seismic safety in India’s infrastructure development by Er Agamoni Das. She noted that recent revisions in Indian seismic codes, particularly IS 1893 (part 1 and Part 5), have introduced substantial changes in seismic force estimation, system classification, and detailing philosophy.
The objective of this webinar, as she explained, was to bridge the gap between theoretical seismic design principles and their implementation in real-world steel structures.
This session aimed to discuss codal provisions, ductility requirements, connection detailing, and performance-based design approaches.

In the opening remarks, Dr. Gupta emphasized to multiple designs always prioritize safety above all other considerations, such as economy or aesthetics. He remarked the structures are subjected to multiple forces during their lifetime, but earthquakes remain uniquely challenging due to their unpredictable and dynamic nature. Each seismic event provides critical lessons that influence future design evolution.

Reflecting on global earthquake experiences, he noted that seismic damage extends beyond structural collapse affecting infrastructure functionality, economic continuity, and community resilience.

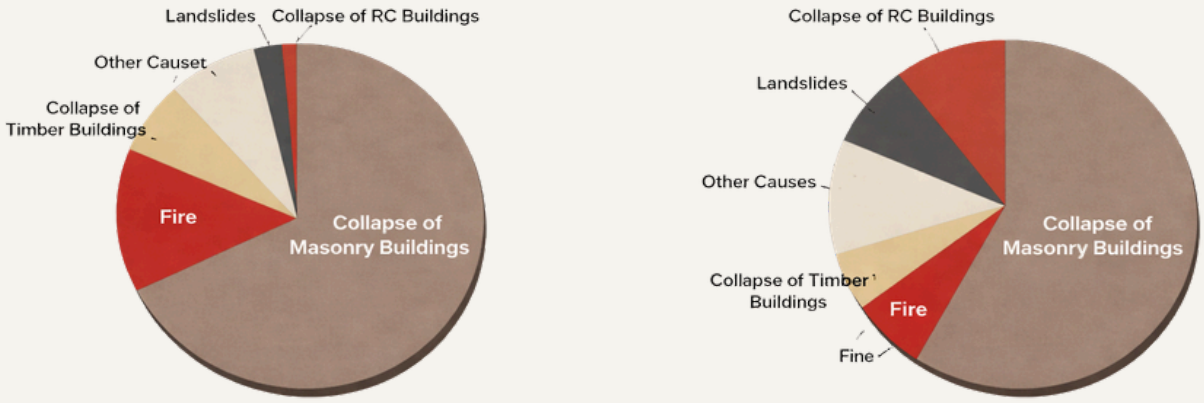

Past Earthquake Performance

Fundamental Virtues of Seismic Steel Design

Dr. Gupta outlined four key attributes governing the seismic performance of steel structures:

1. Strength
2. Stiffness
3. Ductility
4. Structural Configuration

He stressed that while strength and stiffness control elastic response, ductility governs post-elastic behavior and energy dissipation.

Using illustrative examples, he explained that steel structures do not resist earthquakes by remaining rigid, but by deforming in a controlled and predictable manner.

A major portion of the discussion focused on lessons learned from past global earthquakes. Events such as the Northridge (1994) and kobe (1995) earthquakes revealed unexpected brittle failures in steel beam column connections.

Despite the inherent ductility of steel, several welded moment connections fractured prematurely. Investigations identified contributing factors such as:

1. Inadequate weld detailing
2. Low fracture toughness
3. High stress concentration near joints
4. Poor construction quality

These findings triggered significant advancement in connection design philosophy worldwide.

Evolution of Seismic Connection Detailing

Post-earthquake research led to the development of improved seismic connection systems designed to enhance ductility and rotation capacity.

Dr. Gupta discussed various detailing strategies now widely adopted in seismic steel design, including **Reduced Beam Sections, Reinforced Flange Plate Connections, Haunched beam details, and Stiffened end plate systems.**

These innovations are aimed at shifting plastic hinging away from column faces, thereby protecting critical joints from brittle failure.

Capacity Design Approach

The concept of capacity design was emphasized as a cornerstone of modern seismic engineering.

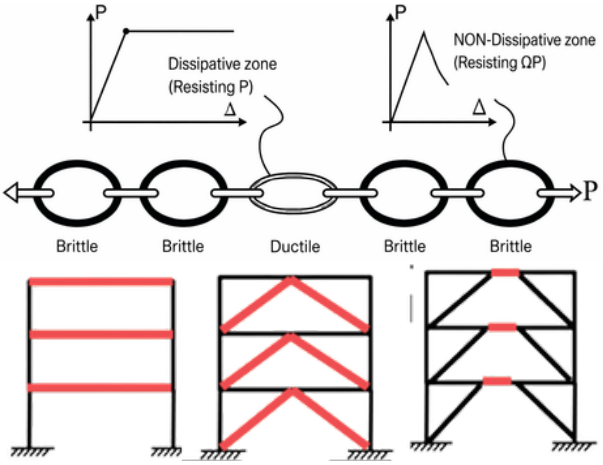

Ductile Fuse Concept

Rather than designing all members to remain elastic, engineers intentionally define ductile “fuse zones” where energy dissipation will occur. Dr. Gupta explained this hierarchy through system behavior:
In the moment resting frames-**beams yield first**
In braced frames-**braces yield first**
In eccentric frames-**links yield first**
All surrounding members are designed stronger to ensure global stability.

Seismic Structural Systems
Dr. Gupta elaborated on the seismic performance of different steel lateral load-resisting systems.
Ordinary Concentrically Braced Frames (OCBF) provide high stiffness but limited ductility.

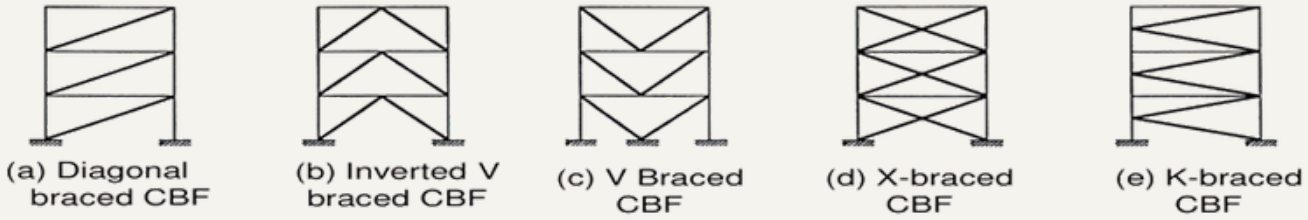

Bracing Systems in OCBF

Special Concentrically Braced Frames (SCBF) improve ductile response through enhanced detailing.
Eccentrically Braced Frames (EBF), however, were highlighted as one of the most efficient systems, incorporating shear links that act as structural fuses to dissipate seismic energy.
He noted that EBF systems are particularly recommended in higher seismic zones due to their superior performance.

Material and Sectional Considerations
With reference to codal provisions, Dr. Gupta explained that material selection significantly influences ductile performance.

He highlighted that **E250** to **E350** steel grades are recommended for ductile members, Higher grades may be used in **non-yielding components, Section compactness** must be ensured.
Plastic and **compact** sections are performed over slender sections to avoid premature local buckling during cyclic loading.

Ductile Behavior and Energy Dissipation
Steel structures survive seismic forces through controlled inelastic deformation, allowing them to withstand the dynamic loads imposed by earthquakes without sustaining permanent damage.
Key mechanism includes **plastic hinge formation, stable cyclic yielding, force redistribution, structural redundancy.**
This ductile response prevents collapse and allows gradual damage progression.

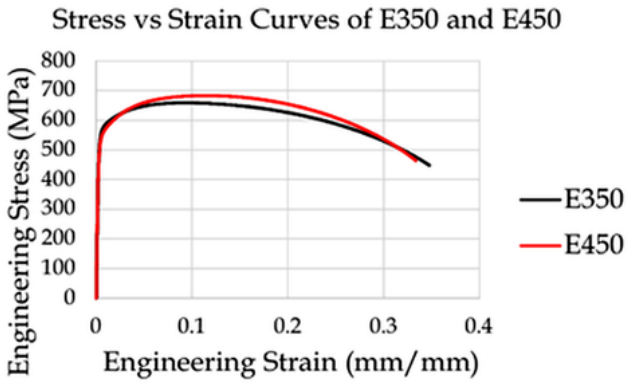

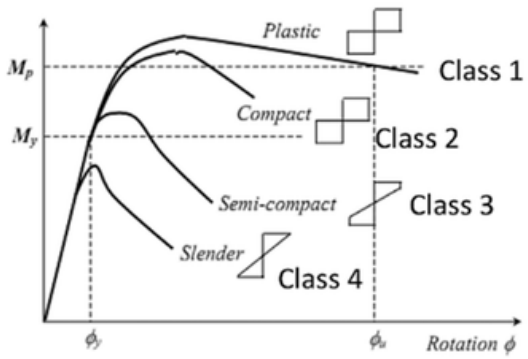

Compactness Criteria

The webinar also reviewed the coordinated application of Indian seismic design standards, including IS 1893, IS 800, and IS 18168. Dr. Gupta highlighted the role of overstrength factors, load combinations, and detailing requirements in ensuring codal compliance and performance reliability.

The session concluded with an engaging Q & A interaction where participants raised practical design queries. Discussion covered topics such as

- Over strength factors in EBF systems
- Brace force distribution requirements
- Connection design economy, slip critical bolting applications.

The session concluded with a vote of thanks.

Webinar by Seismic Academy

What is expected from the webinar?

This webinar will focus on **seismic design and safety of structures and connections**, drawing insights from both **IS 1893**, IS 13920, IS 13935 and **IS 1946**. The session will also highlight **global perspectives** on seismic design to support the development of earthquake-resilient systems.


Credits- https://www.architecturaldigest.in/

Seismic Chronicles: Dhajji Dewari

Kashmir's Quilt Against Quakes

On the morning of **8 October 2005**, at **08:50 local time**, the serene valleys of Kashmir were shattered by one of South Asia's deadliest earthquakes. A **magnitude of 7.6** ruptured the earth beneath the **Azad Jammu and Kashmir** region, its tremors felt across **India, Pakistan, Afghanistan and beyond**. In a fraction of time, homes, schools, and civic structures crumbled; villages and towns lay in ruins; and **thousands of lives were lost**. The quake left more than **2.8 million people displaced,** injuring roughly **1,38,000**, and obliterating much of the built fabric of this mountainous land.

Amid the widespread destruction, a quiet architectural lesson emerged in centuries-old vernacular wisdom.
Dhajji Dewari structures demonstrated remarkable earthquake resilience, surviving where millions of conventional buildings collapsed. It was in the aftermath of this tragedy that the traditional construction technique gained global recognition for its inherent seismic strength.

What is Dhajji Dewari?

The people of the **western Himalayas** developed a uniquely **resilient building system** known as Dhajji Dewari. The term comes from the Persian word dhajji, meaning "quilt patchwork". Combined with Dewari, meaning wall, the term **Dhajji Dewari** describes a wall that looks like quilted patchwork.

Constructed from locally sourced timber, stone or brick and mud mortar, the Dhajji Dewari is a simple construction technology; a timber-framed wall, divided into small masonry panels, infilled with mud mortar. But it is precisely this "patchwork" that makes it a natural ally against earthquakes.

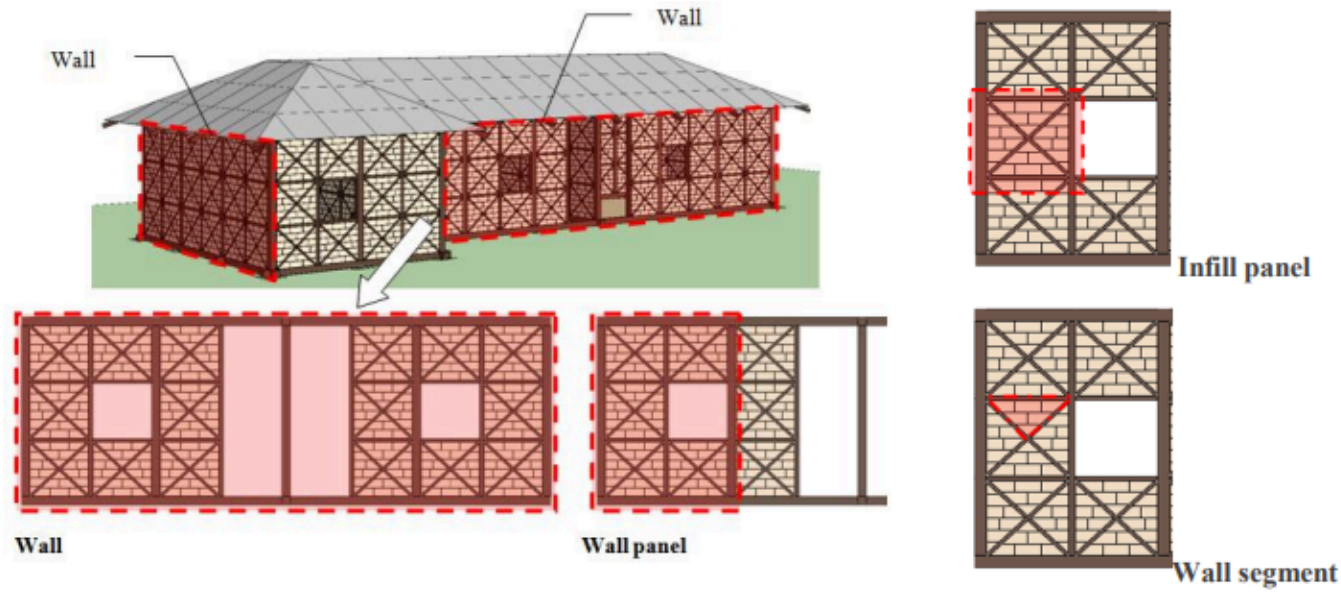

Dhajji Dewari Wall Components, Source - www.iitk.ac.in

Seismic Performance of Dhajji Dewari - K. M. O. Hicyilmaz Associate, Arup Gulf Limited, Dubai, UAE T. Wilcock, C. Izatt, J. da-Silva Ove Arup & Partners, UK R. Langenbach Conservationtech, USA

Design Features of Dhajji Dewari

- **Symmetry and Simplicity:** Planning is usually straightforward: rectangular or square plans with balanced room layouts that distribute loads evenly across the structure. Symmetry prevents torsional forces (twisting) during seismic events, improving stability.
- **Foundation:** The building sits on a stone masonry foundation. A plinth beam, traditionally called dasa, made from strong timber, is anchored securely on this foundation.
- **Timber Frame:** The timber frame forms a continuous, ductile skeleton capable of deforming under seismic motion. During an earthquake, the frame absorbs and redistributes energy, while the masonry infill cracks in a controlled, non-catastrophic manner. As the infill panels are small and separated, they don't lead to total wall collapse, distributing force across the frame and reducing damage.
- **Small Openings:** Large openings can act as weak points under seismic loading, so traditional planning keeps a modest size with timber framing for balanced load distribution.
- **Lightweight Roofs:** Roofs are constructed from timber and locally available materials and are comparatively lightweight. Heavy roofs increase seismic force impact and make buildings more prone to collapse. The lighter the roof, the lower the inertial loads during shaking.

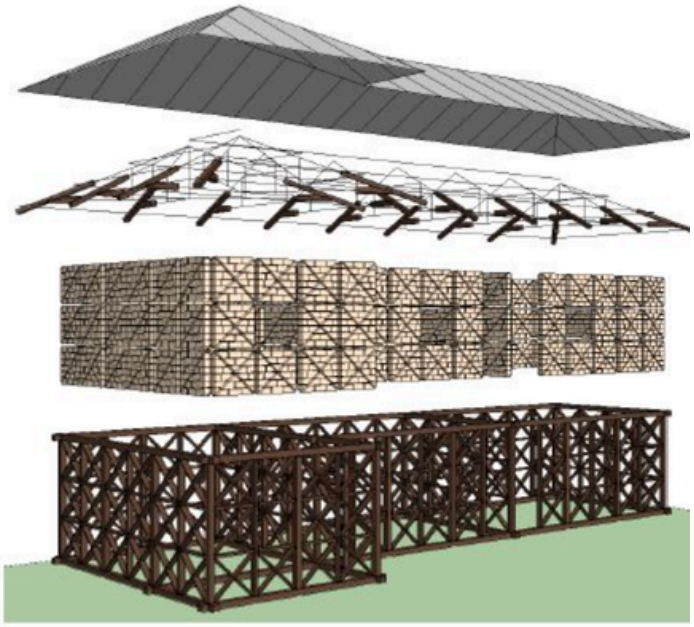

View of Dhajji Dewari Structural Composition
Source- www.iitk.ac.in

Seismic Performance of Dhajji Dewari - K. M. O. Hicyilmaz Associate, Arup Gulf Limited, Dubai, UAE T. Wilcock, C. Izatt, J. da-Silva Ove Arup & Partners, UK R. Langenbach Conservationtech, USA

Reconstruction programmes across the region subsequently encouraged the revival and adaptation of Dhajji Dewari, often combining traditional techniques with improved detailing, better timber connections, and advanced seismic measures. Over 120,000 rural houses were later rebuilt using Dhajji construction in affected areas, with locally available materials to make it cost-effective and environmentally friendly. The reliance on local craft also supports artisans and helps preserve heritage skills while offering a construction approach that is inherently more resilient in a seismic landscape.

Technical Paper

Sloshing Effects in Large Liquid Storage Tanks

By Dr. N. Subramanian (PhD. FNAE, FASCE, FIE) and Dr. H.J. Shah (Ph.D)

1.0 Introduction

Sloshing effects in large liquid storage tanks during earthquakes are a critical design consideration, because excessive sloshing can lead to overtopping, roof damage, uplift of the tank shell, hydrodynamic pressure amplification, and even tank failure. Modern practice manages sloshing through a combination of theoretical modeling, structural detailing, and seismic design provisions.

When an earthquake occurs, the liquid in a large storage tank doesn't move as a single solid block. Instead, it splits into two distinct components: the impulsive mass (the bottom portion that moves rigidly with the tank walls) and the convective mass (the top portion that sloshes back and forth). This separation allows designers to:

- Estimate sloshing wave height
- Compute hydrodynamic pressures
- Evaluate base shear and overturning moments

Most design codes (ACI 350.3, API 650, Eurocode 8, IS 1893-Part 2) are based on this framework.

Managing these sloshing (convective) effects is critical to prevent "elephant foot" buckling, roof damage, or hazardous spills. Engineers use a combination of structural design, internal dampening, and isolation technologies.

2.0 Managing Sloshing Effects

In tanks where sloshing is excessive,

- Baffles or ring plates may be introduced to disrupt wave formation.
- Energy-dissipating devices (less common) reduce convective response.
- Internal columns or partitions (for special tanks) reduce sloshing length.

These are typically used in very large or critical tanks (e.g., LNG tanks).

2.1 Internal Damping: Baffles

Baffles are the most common mechanical way to break up waves and dissipate the energy of the sloshing liquid.

- Horizontal (Annular) Ring Baffles: These are rings attached to the inner wall of the tank near the liquid's surface. As the liquid rises, it must flow over and around these rings, creating turbulence that "drains" energy from the wave.
- Vertical Baffles: Used primarily in rectangular or long horizontal tanks to prevent the buildup of large, longitudinal waves.
- Perforated Baffles: These have holes that allow some liquid to pass through, which is often more effective at damping than solid plates because the resulting "jetting" through the holes creates significant energy-absorbing turbulence.

> **“Seismic safety is achieved through precise impulsive - convective mass modeling”**

2.2 Geometric Management: Freeboard

Large tanks are rarely filled to the very top. Engineers calculate a required Freeboard—the empty space between the liquid surface and the tank roof.

- Wave Height Prediction: Standards like API 650 or Eurocode 8 provide formulas to predict the maximum sloshing wave height based on the site's seismic risk.
- Impact Prevention: If the freeboard is insufficient, the sloshing liquid can hit the roof with enough force to tear it off or buckle the top of the tank wall.

2.3 Structural Decoupling: Floating Roofs

In many oil and chemical tanks, a floating roof sits directly on the liquid surface.

- Suppression: Because the roof rests on the liquid, it acts as a giant weight that physically restricts the free-surface motion.
- Sealing: Flexible seals around the edge of the floating roof prevent the liquid from splashing over the top while allowing the roof to move slightly with the fluid.

2.4 Structural Detailing of Tank Components

Tank Wall and Base

- Walls are designed for combined hydrostatic and hydrodynamic pressures.
- Base slabs and shell-to-base junctions are detailed to resist uplift and rotation.
- Anchorage is provided where uplift demands exceed self-weight.

Roof Systems

- Floating roofs are detailed to accommodate sloshing without binding.
- Fixed roofs are designed to resist sloshing impact or are isolated from the liquid surface

2.5 Foundation and Soil–Structure Interaction

- Flexible foundations can lengthen impulsive periods, reducing force demand.
- Soil–structure interaction is considered for tanks on soft soils.
- Sliding resistance is checked where unanchored tanks are used.

3.0 Advanced Mitigation: Seismic Isolation

Instead of trying to stop the sloshing inside, some modern tanks are built to move with the earthquake to reduce the forces transmitted to the liquid.

Base Isolators: The entire tank is placed on rubber bearings or "sliders" (Lead-Rubber Bearings). These act like shock absorbers, shifting the natural frequency of the tank away from the frequency of the earthquake.

Benefit: This significantly reduces the impulsive force on the walls, though it can sometimes slightly increase the convective sloshing period, requiring a higher freeboard.

4.0 Code-based Seismic Design Provisions

Modern seismic codes manage sloshing by:

- Explicitly defining convective natural periods
- Providing equations for sloshing wave height
- Separately accounting for impulsive and convective forces
- Allowing performance-based checks for critical facilities

> **“Hydrodynamic pressures, uplift, and overturning—addressed through code-driven seismic detailing”**

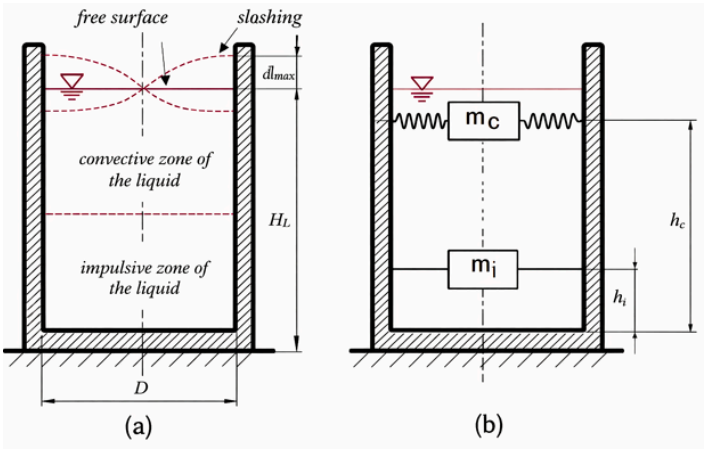

Fig. 1 Actual tank and equivalent simplified spring-mass mechanical model

To design these systems, engineers use the Housner Model (Spring-Mass Analogy). This simplifies the complex fluid dynamics into a mechanical system:

The total liquid mass in the mass is assumed to be divided into two masses and considered independently, as shown in Fig.1.

• Lower Impulsive Mass of liquid, which is not sloshing and remains rigidly attached to the walls.

• The upper Convective Mass of liquid, that is sloshing, is attached to the walls of the tank with a spring stiffness K_C.

API 650 Code

In API 650 Annex E (Seismic Design of Storage Tanks), the "freeboard" is managed by calculating the maximum sloshing wave height. This height determines the minimum clearance required between the liquid surface and the roof to prevent structural damage or overtopping. The calculation is a multi-step process involving the tank's geometry and the seismic characteristics of the site.

> **Designing for controlled sloshing—freeboard governed by quantified wave dynamics.**

1. Calculate the Convective (Sloshing) Period (Tc)

First, you must determine the natural period of the sloshing liquid.

$T_c = K_s \sqrt{D}$ (1)

Where:

- D: Nominal tank diameter (ft).
- K_s: The sloshing period coefficient, which depends on the ratio of the tank diameter (D) to the liquid height (H_L).

It is typically found using: $K_s = \frac{0.578}{\sqrt{\tanh\left(\frac{3.68\,H_L}{D}\right)}}$,

or Fig. 2 given in API 650 code.(2)

2. Determine the Spectral Acceleration (A_f)

Next, find the acceleration coefficient specifically for the sloshing wave. This is based on the site's seismic response spectrum at the period T_C.

If $T_C \le T_L$ (where T_L is the long-period transition period):

$A_f = K\,S_{D1}\left(\frac{1}{T_c}\right)$ (3)

K: Damping coefficient (usually 1.5 to adjust the 5% damped spectrum to the 0.5% damping typical of sloshing liquid), and SD1: Design spectral response acceleration parameter at a 1-second period.

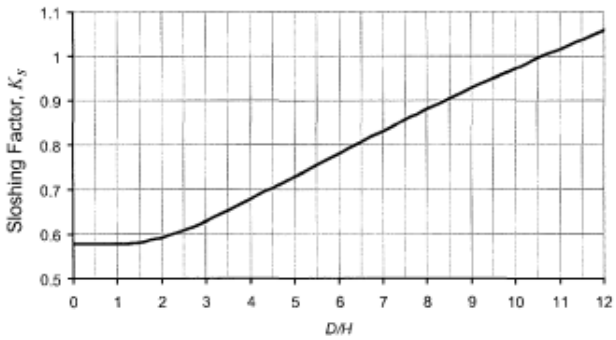

Fig. 2 Sloshing factor K_S

For site-specific analysis, the impulsive spectral acceleration is limited to 1.5g This is based on practical experience and observations of tank behavior

3. Calculate the Sloshing Wave Height (d_S)

The height of the wave above the product design level is calculated as: $d_s = 0.5\,DIA_f$ (4)

Where 'I' is the importance factor

4. Required Freeboard (Fb)

API 650 provides a table (Table E.7, which is reproduced below) for the minimum required freeboard based on the seismic design category and the calculated d_{CS}.

For example, if you have a tank with a 30m diameter and a calculated wave height d_S of 1.2m:

1. For a hazardous material tank (SUG III), one must provide at least 1.2m of freeboard.

Seismic Use Group (SUG)	Minimum Freeboard Required
SUG I (Standard)	Often a percentage of dS or as specified by the purchaser (frequently ~ 0.7 ds).
SUG III (Critical/Hazardous)	Full ds height (the roof must be higher than the maximum predicted wave).

2. For a standard water tank (SUG I) in a lower seismic zone, the code may allow a smaller freeboard (e.g., 0.7m), accepting that the wave might strike the roof in a maximum-intensity event, provided the roof is designed to handle that pressure.

The above calculations are important because:

- **Roof Damage**: If the wave hits a fixed roof, it creates upward pressure that can "pop" the roof-to-shell joint (designed to be frangible).
- **Spillage**: In open-top tanks, insufficient freeboard leads to the immediate loss of contents.
- **Floating Roofs:** For tanks with internal floating roofs, the freeboard calculation must also account for the height of the floating roof seal assembly to ensure it doesn't get crushed against the top angle.

5.0 Performance-Based and Advanced Analysis (Critical Facilities)

For nuclear, LNG, or lifeline tanks:

- Nonlinear time-history analysis with fluid–structure interaction is used.
- CFD-based sloshing simulations assess wave impact and roof interaction.
- Design targets include no loss of containment even under extreme shaking.

6.0 Seismic Sloshing Provisions in Different Codes

In the calculation of the seismic effects, simple equivalent mechanical models are used to investigate tank-liquid systems. The most widely used model adopted in various international codes is the one based on spring-mass modeling proposed for rigid tanks by G.W. Housner (See Fig. 1), which was later modified and extended for flexible tanks.

Some of the seismic sloshing provisions of different codes are compared in Table 1.

Table 1 Comparison of seismic sloshing provisions of different codes

Aspect	ACI 350.3 / ASCE 7	API 650 (App. E)	Eurocode 8 (EN 1998-4)	IS 1893 (Part 2)
Liquid model	Impulsive + convective	Impulsive + convective	Impulsive + convective	Impulsive + convective
Sloshing period	Closed-form (Housner-based)	Similar to ACI	Explicit modal expressions	Similar to ACI
Sloshing height	Explicit formula	Explicit	Explicit (often higher)	Explicit
Roof interaction	Checked explicitly	Checked	Explicitly addressed	Limited guidance
Anchorage	Required if uplift > weight	Strong emphasis	Explicit	Explicit
Damping (sloshing)	~0.5%	~0.5%	0.5–1%	~0.5%
Performance philosophy	Life safety / containment	Industry-based safety	Reliability-based	Prescriptive

From the above table, it is seen that all modern codes are mechanically consistent, but differ in:

- Conservatism of sloshing height
- Treatment of roof–liquid interaction
- Detailing and anchorage requirements

7.0 Example Calculation – Ground-Supported Circular Tank

Given

- Tank type: Ground-supported RC tank
- Inside Radius, R=15 m, Hence, Diameter D=30 m
- Liquid height, H_L =10 m
- Design peak ground acceleration, C_a =0.15g (Typical for Moderate Seismic Zones)
- Importance factor, I = 1.0
- Liquid density = 1000 kg/m3

Step 1: Determine the Convective Period (T_c)

The convective period depends on the ratio of the diameter to the liquid height.
Ratio D/H_L =30/10 =3.0

According to ACI 350.3, the formula for T_c in a circular tank is:

$$T_c = \frac{2\pi}{\sqrt{3.68g\tanh\left(\frac{3.68H_L}{D}\right)}}\sqrt{D} \quad (5)$$

Using the ACI frequency factor (Cc) for D/H_L = 3.0:
From ACI 350.3, Figure 9.3.4(b), for D/H_L = 3.0, the factor is 0.63 that gives approximately 0.63 x 1. 811 = 1.14 in metric units.
T_c= 1.14√30 = 6.24 sec.

Step 2: Determine Convective Spectral Acceleration (S_{ac})

For sloshing, ACI 350.3 typically uses 0.5% damping. S_{ac} is calculated based on the site response spectrum at period T_C.

If we assume a standard spectral shape where S_{ac} = 1.5 C_a/T_C for long periods:
S_{ac} = 1.5 x 0.15g / 6.24 = 0.036 g

Step 3: Calculate the Sloshing Height (ds)

The sloshing height is the maximum vertical displacement of the liquid surface at the tank wall. The ACI 350.3 formula is:

$$d_s = 0.5DIS_{ac}$$

Hence,
d_S=0.5×30×1.0×0.036=0.54 m

Design implication

- Minimum freeboard ≥ 0.54 m
- Add margin for uncertainty (often 20–30%), hence, adopt a minimum freeboard =1.3 x 0.54 = 0.70 m

Note that if Freeboard < 0.54m, the design of the roof slab should be designed to withstand the "slapping" or upward pressure of the liquid during an earthquake, and the impulsive forces must be increased to account for the restricted sloshing.

Impulsive Base Shear

Total liquid mass:

$$m = \rho\pi R^2 H = 1000 \times \pi \times 15^2 \times 10 = 7.068 \times 10^6 \text{ kg}$$

7.068 ×106×0.00981= 69337 kN

Determine the Convective Mass Ratio (W_C / W_L)

Using the ratio D/H_L =30/10 =3.0, using the ACI 350.3 formula for circular tanks:

$$\frac{W_c}{W_L} = 0.23\left(\frac{D}{H_L}\right)\tanh\left(3.68\frac{H_L}{D}\right)$$

$$\frac{W_c}{W_L} = 0.23 \times 3 \times tanh\left(\frac{3.68}{3.0}\right) = 0.58$$

The above ratio will normally be about 0.55 to 0.65.
Convective Weight, W_C = 0.58 x 69337 = 40264 kN

Calculate Convective Base Shear (V_C)

The base shear for the convective component is defined by the formula:

$$V_c = S_{ac}IW_c$$

From our previous step, we calculated the convective spectral acceleration, S_{ac} = 0.036g

Convective base shear:

$$V_c = 40264 \times 1 \times 0.036\,\text{g} = 1409.5\,\text{kN}$$

(This governs shell stresses and anchorage.)
Determine the Impulsive Mass Ratio (W_i / W_L)
Using the ACI 350.3 formula,

$$\frac{W_i}{W_L} = \frac{\tanh\left(0.866\frac{D}{H_L}\right)}{0.866\frac{D}{H_L}} = \frac{\tanh(0.866\times3)}{0.866\times3} = 0.381$$

Calculate Impulsive Weight (W_i)

Using the total liquid weight calculated previously (W_L = 69,337kN):
W_i =0.381 x 69337 =26,417 kN

Verification (Mass Balance Check)
In a simplified seismic model, the sum of the impulsive and convective masses should approximately equal the total mass of the liquid.
W_i = 26,417kN
W_C = 40,264 kN
Total (W_i + W_C): 66,681kN

Note: The sum is slightly less than W_L of 69,337 kN (approx. 96%) because ACI 350.3 accounts for higher-order sloshing modes that represent a very small fraction of the remaining mass.

Impulsive Base Shear (V_i)
To calculate the Impulsive Base Shear (V_i) and the Total Design Base Shear (V), we apply the response modification factors (R) prescribed by ACI 350.3-20. These factors account for the ductility and energy-dissipation capacity of the reinforced concrete structure.
For a "rigid" or "short-period" tank, the impulsive component corresponds to the constant acceleration region of the seismic response spectrum.

Design Spectral Acceleration (S_{ai}): For a peak ground acceleration (C_a) of 0.15g, the spectral acceleration is typically amplified by a factor of 2.5 in the plateau region.

$$S_{ai} = 2.5C_a = 2.5 \times 0.15 = 0.375\,\text{g}$$

Response Modification Factor (R_i): For a ground-supported, anchored reinforced concrete tank, ACI 350.3 Table 4.1.1(a) specifies R_i = 3.25.
Importance Factor (I): 1.0
Calculation of Impulsive Base Shear (V_i)
The formula for the impulsive base shear is:

$$V_i = \frac{S_{ai}\, I\, W_i}{R_i} = \frac{0.375 \times 1 \times 26417}{3.25} = 3048\ \text{kN}$$

Total Design Base Shear (V)
The total base shear is not a simple sum of the impulsive and convective parts because their peaks occur at different times. ACI 350.3 requires the SRSS (Square Root of the Sum of the Squares) combination.
Impulsive Shear (V_i): 3,048. kN
Convective Shear (V_C): 1409 kN

$$V = \sqrt{V_i^2 + V_c^2} = \sqrt{3048^2 + 1409^2} = 3358\ \text{kN}$$

This total shear force, 3358 kN, is the lateral force used to design the tank's wall-to-foundation connection and to check for sliding and overturning stability.

> **"Anchorage and shell–base detailing is engineered for reliable impulsive and sloshing force transfer"**

8. 0 Summary and Conclusions
During seismic excitation, liquid storage tanks respond through a combined impulsive–convective mechanism. The impulsive component moves in unison with the tank wall and governs hydrodynamic pressures, base shear, and overturning moment, whereas the convective component represents sloshing of the free surface and controls wave height and roof interaction. Modern design codes such as ACI 350.3, API 650, Eurocode 8, and IS 1893 (Part 2) explicitly account for these mechanisms by assigning distinct natural periods, damping ratios, and force contributions. Adequate freeboard, proper anchorage, and detailing at the shell–base junction are essential to ensure containment integrity under earthquake loading.

Thus, the sloshing effects in large liquid storage tanks are managed by:

- Separating impulsive and convective liquid behavior
- Providing adequate freeboard and roof clearances
- Designing tank walls, base, and anchorage for hydrodynamic effects
- Using baffles or damping measures when necessary
- Following code-specified seismic liquid–structure interaction models

This integrated approach ensures containment integrity, operational safety, and seismic resilience of liquid storage tanks.

References

1. Housner, G.W. (1957)."Dynamic pressures on accelerated fluid containers", Bulletin of the Seismological Society of America, Vol. 47, No. 1, pp. 15–35. https://doi.org/10.1785/BSSA0470010015
2. A. S. Veletsos (1984). Seismic Response and Design of Liquid Storage Tanks, Guidelines for the Seismic Design of Oil and Gas Pipeline Systems, Technical Council on Lifeline Earthquake Engineering ASCE, 1984.
3. EN 1998-4(2006), Eurocode 8 – Design of Structures for Earthquakes Resistance, Part 4 –Silos, Tanks and Pipelines.
4. IS 1893 (Part 2): 2014 Criteria for Earthquake Resistant Design of Structures, Part 2: Liquid Retaining Tanks, Fifth Revision (Reaffirmed 2019), Bureau of Indian Standards (BIS), New Delhi.
5. API Standard 650 (January 2021) Welded Tanks for Oil Storage, Annex E: Seismic Design of Storage Tanks, 13th Edition, American Petroleum Institute (API)
6. ACI CODE-350.3(2020) Code Requirements for Seismic Analysis and Design of Liquid-Containing Concrete Structures and Commentary, American Concrete Institute (ACI)
7. ASCE/SEI 7-22: Minimum Design Loads and Associated Criteria for Buildings and Other Structures, American Society of Civil Engineers (ASCE).Chapter 15.
8. Shah, H.J. Reinforced Concrete, Vol. II, 8th Revised and Enlarged Edition, Charotar Publishing House Pvt. Ltd., Anand, Gujarat, 2023, 776 pp.

About the Authors

Dr. N. Subramanian
Ph.D. FNAE, FASCE, FIE

Dr. N. Subramanian, PhD. FNAE, FASCE, FIE is a highly respected structural engineer, prolific author, and mentor, currently based in Maryland, USA, with over 48 years of professional experience spanning consulting, research, and teaching. He is widely recognized for his exceptional contributions to the field of structural engineering, both in India and internationally. He was awarded the 2024 Edmund Friedman Professional Recognition Award of the American Society of Civil Engineers, ACCE(I)'s Gourav Award, ICI's 'Life Time Achievement Award' and many other awards for his contributions towards Structural Engineering. He is the author of 25 books and over 320 papers, including the famous books on 'Design of Steel Structures', 'Design of RC Structures', 'Principles of Space Structures' and the recent 'Building Materials, Testing and Sustainability'. (Email - drnsmani@yahoo.com)

Dr. H. J. Shah
Ph.D

Dr. H. J. Shah, Ph.D., is a retired associate professor of M. S. University of Baroda (Gujarat, India), with a teaching experience of 37 years, and a well-recognized consulting structural engineer with over 42 years of Professional experience. He is an author of the highly acclaimed books 'Reinforced Concrete Volume I (in two parts) and 'Reinforced Concrete Volume II. A coauthor with the late Prof. S. B. Junnarkar for three books on analysis. A special publication on Six-storeyed building - EQ 26 – by Dr. H. J. Shah and Dr. S. K. Jain is an extremely referred document since 2003, available on the NICEE website. He had also worked in the post-earthquake scenario to impart special consultancy in the field of structural damage assessment, retrofitting measures and rehabilitation of damaged structures. He remained as a registered consultant to GWSSB (Gujarat Water Supply and Sewerage Board) from 2006 to 2019.
(Email- hjshah-appmech@msubaroda.ac.in)

Non-structural connections are part of Seismic standard

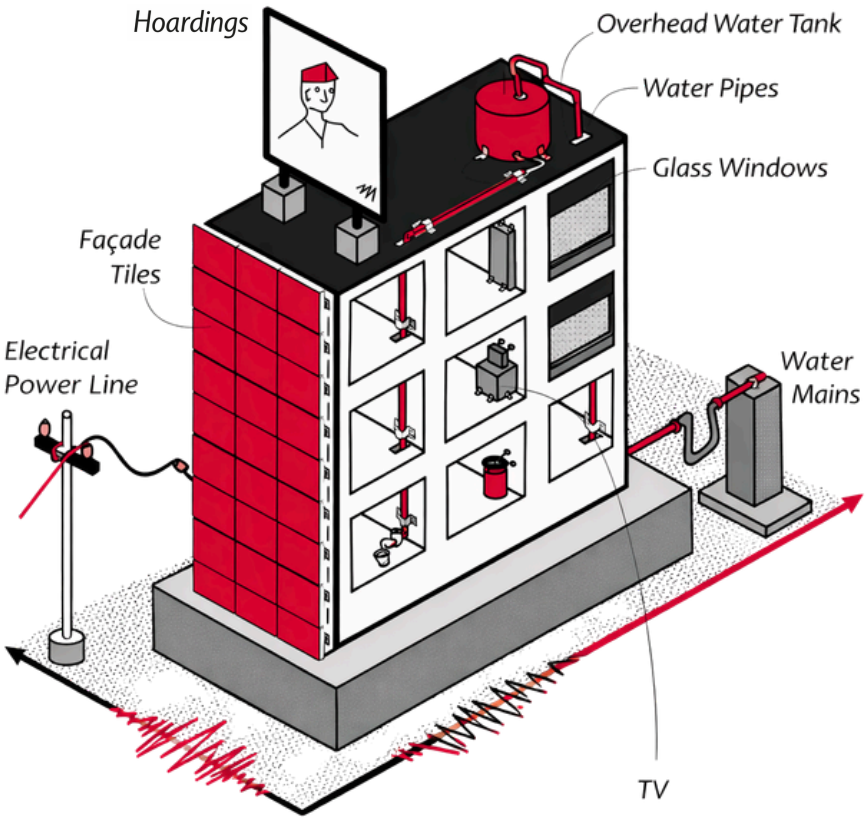

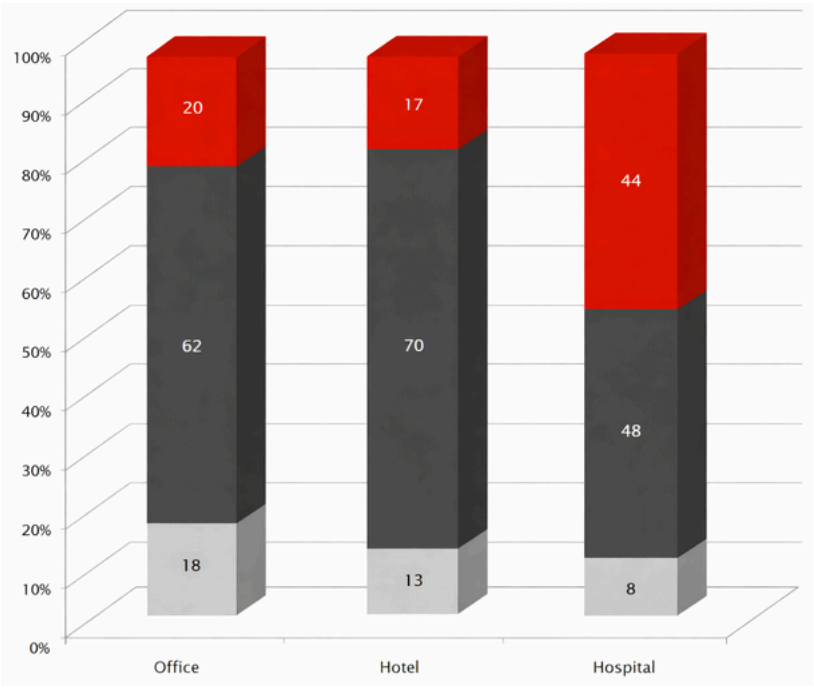

Architectural Elements and Utilities

Architectural elements and utilities (AEUs) in all structures shall be designed to remain fully functional in the aftermath of the design earthquake shaking.

Contents

Non structural

Structural

Technical Paper

Numerical Analysis of a Long Bridge with Tall Piers under simultaneous action of Seismic Excitation and Moving Train

Abhishek, Post Graduate Student, Civil Engng. Dept., IIT Guwahati, India
Prinza Priya Loying, Sumantra Sengupta, Research Scholar, Civil Engng. Dept., IIT Guwahati, India
and Dr. Anjan Dutta, Professor, Civil Engng. Dept., IIT Guwahati, India

Abstract

The study is related to the assessment of performance of a long multi-span railway bridge with through type open web superstructure and located in the highest seismic zone of India under simultaneous action of earthquake and moving train. Piers are tall with heights varying from 60 to 140 m and are expected to show significant amplification of seismic response at pier top level. In a long bridge, spatial variation in the input seismic excitation should be considered; **the effect of this variation at different pier foundation levels on the overall seismic performance of the bridge must be assessed.** A detailed finite element model with soil-structure interaction is considered. Asynchronous ground motions are modelled using conditional simulation that accounts for the coherency losses and a time delay of arrival with change in phase as well as amplitude of the earthquake signals from origin to the spatial points of interest along the bridge. Multi-support excitation of the bridge is performed by converting the acceleration time history to displacement time history. A 27 DOF vehicle model is used to assess the safety of a moving train, while the bridge is simultaneously acted upon by an earthquake shaking. The responses at different pier locations for the synchronous and asynchronous motion are evaluated, and the requirement of asynchronous input in multi-support excitation for a long bridge with tall piers is observed to be significant for the assessment of safety of running vehicle.

Keywords

Long bridge with tall piers, Seismic performance, Conditional Simulation, Asynchronous motion, multi-support excitation, Vehicle model

1. Introduction

Long bridges may have multiple supports and the abutments at two ends as well as intermediate piers, are quite likely to be at a significant distance apart. During seismic excitation, the expectation of the same earthquake motion at every support point is thus unlikely to be accurate, as during its propagation, the earthquake motion undergoes reflection, refraction, and losses its coherent nature, resulting in a whole different motion when measured at different points for the same earthquake event.

The spectral properties of ground motion get altered because of (a) wave passage effects which is due to the time shifts in the arrival of the seismic waves at the supports (Adanur et al.[1]) (b) the incoherence effect which is due to extended source effect in which different frequencies in the relative geometry of the source and site produce different time shift (Konakli and Kiureghian [2]) (c) the local soil effect which causes scattering (reflection, refraction etc) of waves by inhomogeneity along the travel path. The asynchronous ground motions were started being analyzed after the installation of dense instrument arrays since 1979 with El Centro differential arrays. Before this, the spatial variation of the motions was attributed to the wave propagation effect only (Bogdanoff et al. [3]).

Numerous researchers have done work on spatial variation of seismic ground motion and its application on long span structures. In general, the spatial variations of seismic ground motions are evaluated from data recorded at dense instrument arrays. Zerva and Zervas [4] studied the estimation of coherency from the recorded data and discussed on its interpretation. Some empirical and semi-empirical coherency models based on the recorded data, their validity as well as limitations and the effect of coherency on the seismic response of extended structures were studied. Lavorato et al. [5] studied the nonsynchronous seismic ground motion generated at different foundation point of a long span bridge. Basu et al. [6] developed a framework which accounts for both phase variability and amplitude variability of spatially varying ground motion. For assessment, a definition of target spectrum based on the direction of arrival was explored. The effect of choice of coherency model on the simulated spatially varying ground motion was investigated. ("Practical coherency model suitable for near- and far-field earthquakes ...") Seismic response analysis of structures subject to multi-support excitation has been carried out by various methods like modal analysis (Berrah [7]), modified response spectrum method (Kiureghian and Neuenhofer [8]), Monte Carlo simulation (Mirzabozorg et al. [9]), random vibration analysis (Zhang et al. [10]), etc. Balamonoca et al.[11] used a deterministic approach using proper orthogonal decomposition vector (POD) or proper orthogonal mode to analyse the response of the structure subjected to multisupport excitation. Experimental and numerical studies show that the relative displacement of the bridges tends to increase, causing pounding when subjected to spatially varying earthquakes (Li et al.[12]). Nguyen et al. [13] established a simulation procedure for vehicle–substructure dynamic interactions. Each vehicle is modelled as a multi-axle double-layer of a mass-spring-damper system having 27 DOFs, and the bridge is modelled using the finite element method. The wheel–rail dynamic interaction model couples the train subsystem with the track subsystem at the wheel–rail interfaces. rigid contact assumption, where the wheel displacement is considered identical to that of the bridge or rail beneath it, implying continuous contact without separation (Yang et al. [14]) has been popularly used by many researchers.

It is understood from the literature study that the asynchronous motion will cause enhanced relative motion in pier top in multi support long span bridge compared to synchronous motion. In railway bridge, this effect causes relative displacement of the continuous rail on which trains are moving. "In the present study, development of asynchronous motion and its effect on long span bridge with multi support arrangement has been presented." ("Civil-Comp Conference Proceedings") In railway bridge, the continuous track alignment undergoes lateral movement during seismic excitation. The train speed depends on the track curvature in addition to the other factors. The relative effect of track curvature between synchronous and asynchronous ground movement has been studied for a long railway bridge with tall piers and located in the highest seismic zone of India. A 27 DOF vehicle model with rigid contact assumption has been considered in the present study. The seismic performance of bridge-vehicle system has been studied to examine the importance of synchronous and asynchronous ground movement in terms of safety of the overall system.

2. Finite Element Modelling of the Considered Bridge

The bridge under consideration is a railway bridge with an open web girder superstructure. The bridge is in Manipur, India, which has the highest seismicity in the country. The total length of the considered bridge is 703 m, which comprises of eight simply supported spans. It has two 69 m span with a through-type truss girder, five numbers of 103.5 m span with a through-type truss girder and a plate girder span of 28.5 m. The bridge consists of seven intermediate annular piers of height ranging from 60 metres to 141 metres.

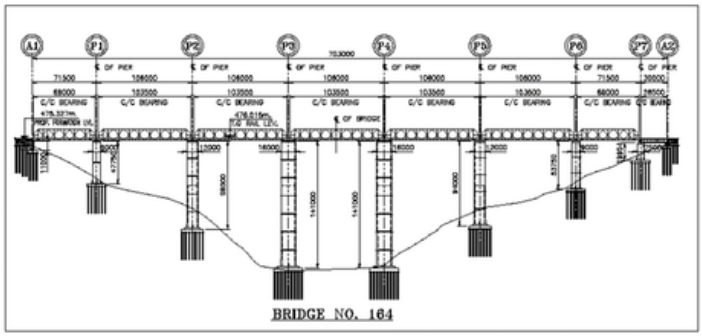

Fig. 1 Tall Long Railway Bridge in Manipur

The tall Piers resting on Pile foundations are flexible and must be modelled appropriately to represent their actual behaviour. The bridge is supported on a group of piles with a diameter of 1.5 meters and a length varying between 22 meters to 30 meters at the respective locations (Figure 1). Members of the superstructure with different sectional geometries are modelled in section designer. Beam elements are used to model the piers, piles, while plate elements are used to model the pile cap. The superstructure is also modelled using beam elements, wherein appropriate releases are made to ensure only axial degrees of freedom to members of the truss and rotational degrees of freedom are released for stringers and cross girders to ensure shear transfer only. The through-type truss girder and plate girder spans are simply supported, and boundary conditions are imposed with help of body constraints in SAP 2000 Nonlinear. The near-field soil is modelled using Beam on Winkler Foundation, where soil elements are modelled as discrete non-linear springs as specified in API 2008 [15]. The soil resistance in the lateral and axial direction of the pile is summarised as a P-y curve to represent the relationship between the lateral resistance of soil and pile displacement, a t-z curve to represent the relationship between shaft skin frictional force and relative movement of the pile with respect to the soil, Q-z curve to represent the mobilized tip bearing capacity and settlement. "The detailed finite element model of the considered bridge, along with the soil-pile system, is shown in Fig. 2 ("Civil-Comp Conference Proceedings")

3. Multi-Support Excitations Using the Displacement Input Method

Multi-support excitation in SAP 2000 Nonlinear is performed by converting acceleration time history to displacement time history, while the time step is reduced to 1/10th of acceleration time history.

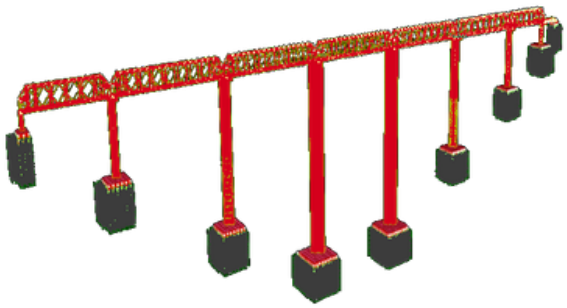

Fig. 2 Finite Element Model of the Bridge with Near-Field Soil Springs

The P-y spring is positioned along with two orthogonal directions on the horizontal plane and is connected to the pile at discrete points over its length. The converted displacement time history and applied as joint/ground displacement at each fixed end of the two-jointed P-y spring (Fig. 3).

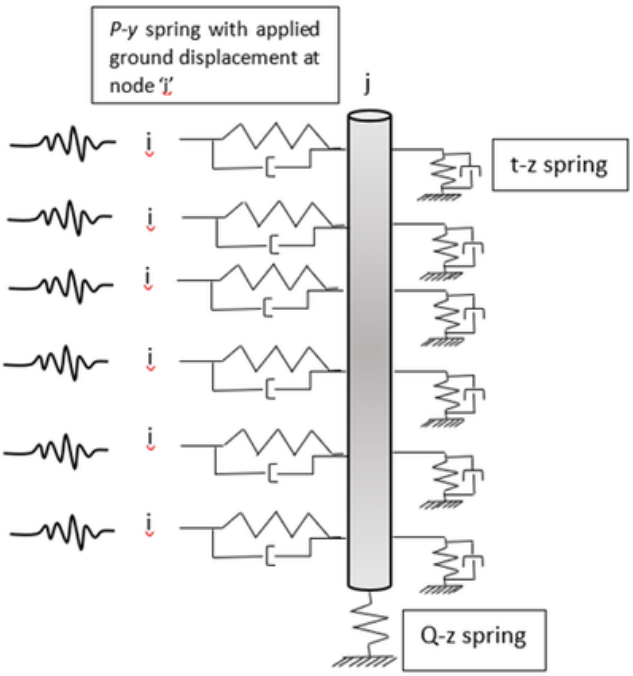

Fig. 3 Schematic diagram of Pile with input ground displacement at 'ith' node

The structural response that is obtained from displacement-based input is the total displacement response, whereas for acceleration-based input, the response that is obtained is the relative displacement response. The equations of motions that are solved by SAP 2000 for performing multi-support excitation are:

$$\begin{bmatrix} M_{ss} & M_{sb} \\ M_{sb} & M_{bb} \end{bmatrix} \begin{Bmatrix} \ddot{u}_s \\ \ddot{u}_b \end{Bmatrix} + \begin{bmatrix} C_{ss} & C_{sb} \\ C_{sb} & C_{bb} \end{bmatrix} \begin{Bmatrix} \dot{u}_s \\ \dot{u}_b \end{Bmatrix} + \begin{bmatrix} k_{ss} & k_{sb} \\ k_{sb} & k_{bb} \end{bmatrix} \begin{Bmatrix} u_s \\ u_b \end{Bmatrix} = \begin{Bmatrix} 0 \\ R_b \end{Bmatrix} \quad (1)$$

where, $\ddot{u}_s$,$\dot{u}_s$,u_s are the vectors representing the motion of the superstructure in the absolute coordinate system; $\ddot{u}_b$, $\dot{u}_b$, u_b are the vectors representing ground motion in the absolute coordinates;

M_{ii}, C_{ii} , k_{ii} are the mass, damping and stiffness matrices. The meaning of subscripts like ss, bb and sb is the degrees of freedom of the superstructure, base, and their coupled term. R_b is the lateral reaction at the nodes of the foundation. Considering the expanded form of the first row of Equation 1, we get

$$M_{ss}\ddot{u}_s + C_{ss}\dot{u}_s + k_{ss}u_s = -(M_{sb}\ddot{u}_b + C_{sb}\dot{u}_b + k_{sb}u_b) \quad (2)$$

In the case of the lumped mass model, all non-diagonal terms are zero, thus M_{sb} is equal to zero. The damping term $-C_{sb}\dot{u}_b$ can be neglected (Computers and Structures [16]). So, Equation 2 can be written as

$$M_{ss}\ddot{u}_s + C_{ss}\dot{u}_s + k_{ss}u_s = -k_{sb}u_b \quad (3)$$

where u_b is the vector of ground motion in terms of displacements; $-k_{sb}u_b$ is the force experienced by the superstructure for the ground motion in the absolute coordinates. Equation 3 is the displacement-based input model for the analysis of a structure under ground motion.

4. Vehicle Model

In this study, the train model considered comprises of a locomotive and wagons. The number of wagons is chosen in such a way that a large part of the bridge remains loaded. The car body has a total of 5 degrees of freedom (DOFs): vertical, lateral, rolling, yawing and pitching. Similarly, both the front and the rear bogies are assigned 5 DOFs each, while the four-wheel sets of the vehicle are assigned 3 DOFs each. Thus, the 3D vehicle model of the wagon has 27 DOFs. The vehicle model along with the axle spacing and loads are shown in Fig.4 (Nguyen et al. [13]).

The rigid contact algorithm adopted in this study is based on the formulation proposed by Yang et al. [14].

5. Seismic Analysis of the Long Span Bridge for Synchronous and Asynchronous Input Motion

In the present study, two earthquake records with different peak accelerations, frequency contents and durations have been selected as input motion for the time-history analysis of the considered bridge. These recorded earthquakes are Koyna (1967): Comp – Longitudinal and Elcentro (1940): 180-degree component. These input earthquake motions have been converted to a spectrum compatible with respect to the design spectrum for DBE (5% damped) as presented in IS: 1893 [15]. These spectrum compatible time histories are used as synchronous input motion. The conditional simulation of earthquakes that vary spatially using the procedure that has been developed by Fenton et al. [16] is adopted in this study and is used as asynchronous input motion.

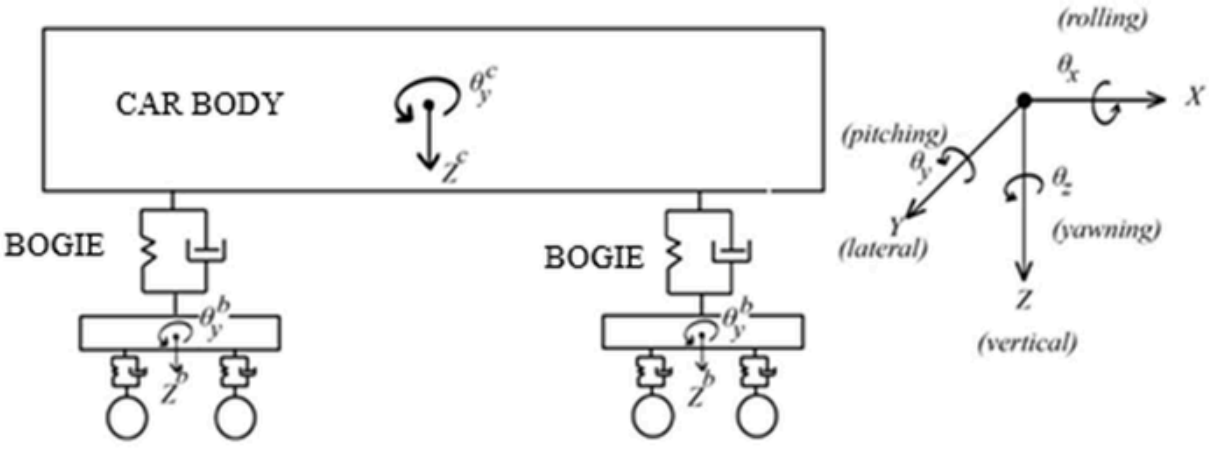

Fig. 4 Vehicle Model with 27 Degrees of Freedom

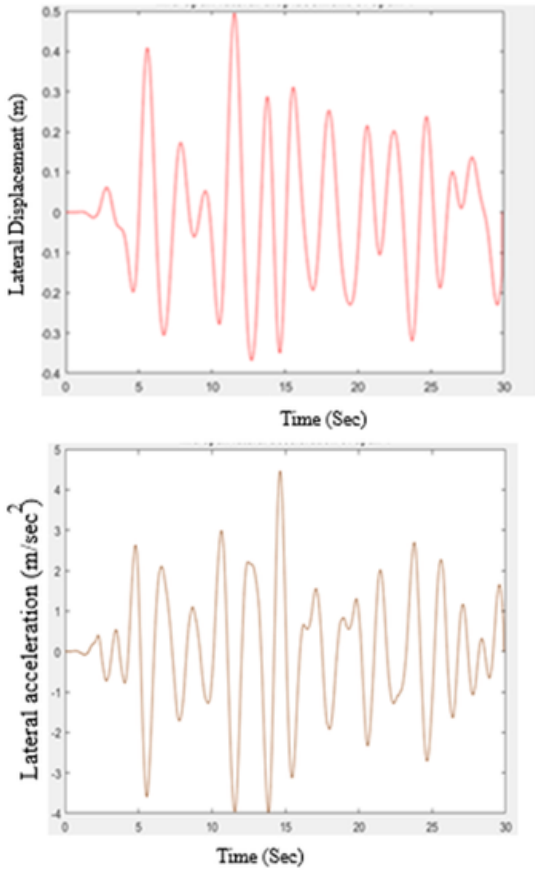

Fig. 5 Lateral displacement and acceleration of span P2-P3 under Elcentro excitation with no train on bridge

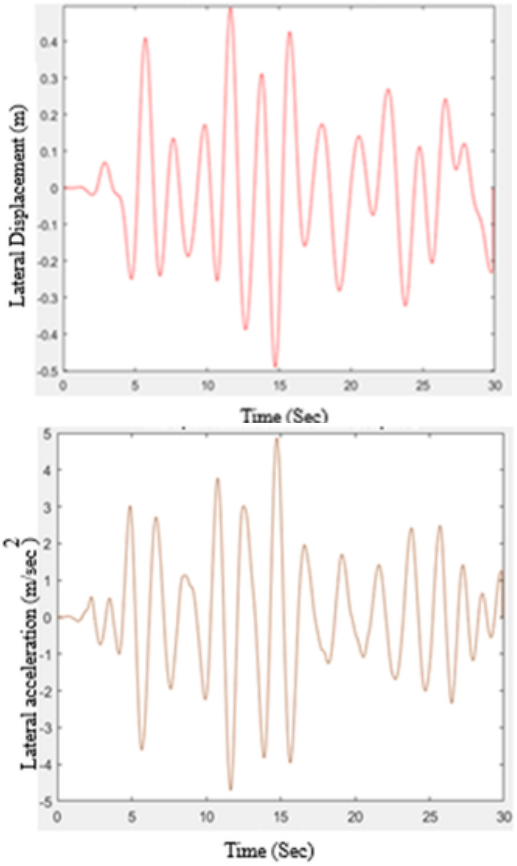

Fig. 6 Lateral displacement and acceleration of span P3-P4 under Elcentro excitation with no train on bridge.

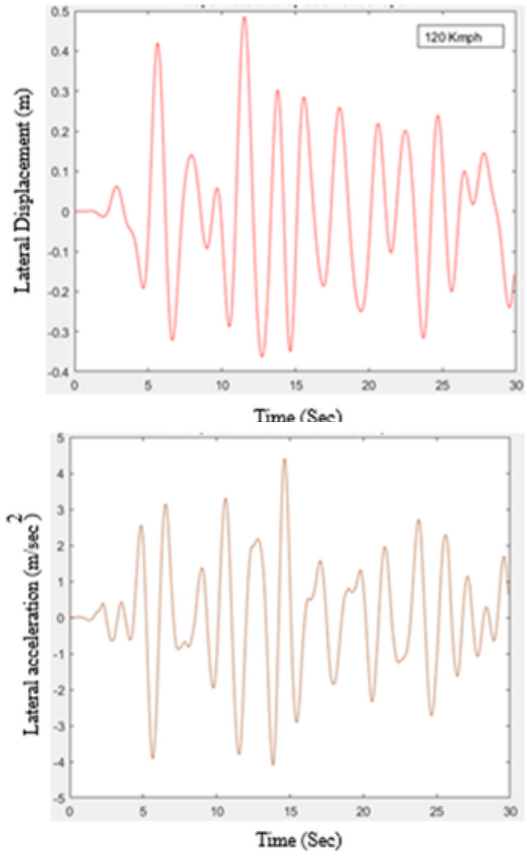

Fig. 7 Lateral displacement and acceleration of span P2-P3 under Elcentro excitation with train moving at 120 kmph.

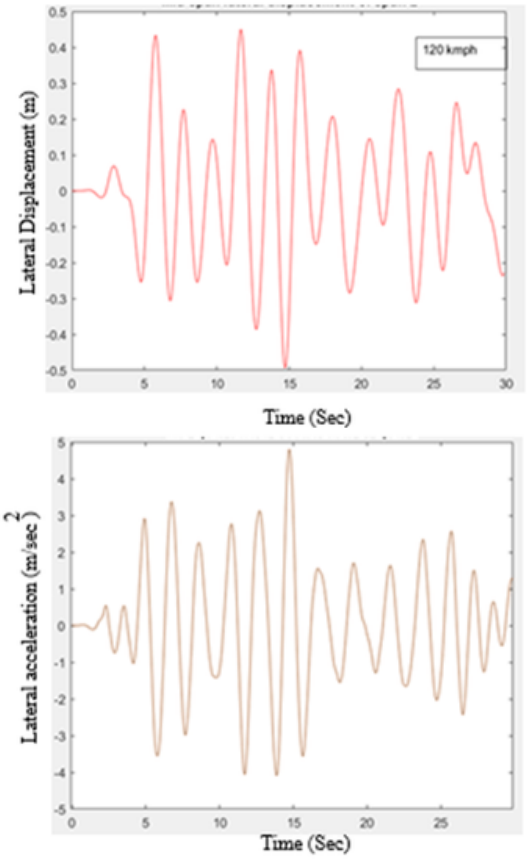

Fig. 8 Lateral displacement and acceleration of span P3-P4 under Elcentro excitation with train moving at 120 kmph.

5.1 Comparison of Responses at Pier Top

The maximum response value at the bridge mid span for different velocities of train for both the cases is shown in Table-1. A few typical time history plots of lateral acceleration and displacement of the bridge at mid span are shown in figures 5-8. It is observed that the bridge structure with a train shows a lesser response in comparison to the case where there is no train and the structure is subjected to seismic excitation alone.

Table 1 Response of Bridge Under Elcentro Excitation for Various Cases

Elcentro Earthquake					
Response at mid span	Span no.	No train condition	With train		
			Speed of train (kmph)		
			60	80	120
Lateral displacement(m) (Synchronous)	P3-P4	0.5049	0.4895	0.4923	0.4955
	P2-P3	0.4930	0.4898	0.4903	0.4919
Lateral displacement (m) (Asynchronous)	P3-P4	0.4587	0.4483	0.4512	0.4529
	P2-P3	0.4326	0.4283	0.4298	0.4310
Lateral acceleration (m/s^2) (Synchronous)	P3-P4	4.4648	4.3720	4.3941	4.3971
	P2-P3	4.8687	4.8175	4.8517	4.8532
Lateral acceleration (m/s^2) (Asynchronous)	P3-P4	4.1693	4.0289	4.1092	4.1461
	P2-P3	4.3278	4.2434	4.2473	4.3048

In the present analysis, span 2 exhibits the highest lateral displacement, which may be attributed to the greater height of pier 2 and pier 3, resulting in increased flexibility. Furthermore, the absolute response under synchronous excitation is observed to be higher than in the asynchronous case.

Table 2 Response of bridge under Mexico earthquake for various cases

Mexico Earthquake					
Response at mid span	Span no.	No train condition	With train		
			Velocity of train (kmph)		
			60	80	120
Lateral displacement (m) (Synchronous)	P3-P4	0.4236	0.4147	0.4212	0.4234
	P2-P3	0.3907	0.3850	0.3897	0.3902
Lateral displacement (m) (Asynchronous)	P3-P4	0.3855	0.3779	0.3818	0.3846
	P2-P3	0.3390	0.3311	0.3340	0.3369
Lateral acceleration (m/s^2) (Synchronous)	P3-P4	4.3113	4.1274	4.2025	4.2514
	P2-P3	4.8925	4.8019	4.8468	4.8902
Lateral acceleration (m/s^2) (Asynchronous)	P3-P4	3.9498	3.8717	3.885	3.9161
	P2-P3	4.4164	4.3219	4.3866	4.4054

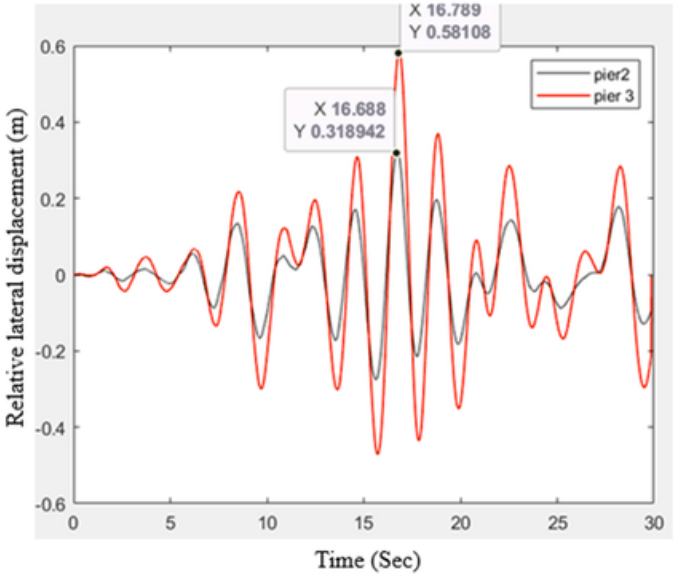

Fig. 9 Relative displacement between Pier 2 (P2) and Pier 3 (P3)

5.2 The relative displacement of adjacent piers

The bridge under study exhibits geometric irregularity due to varying pier heights. Pier-2(P2) and Pier-3(P3), both measuring 98 m and 141 m respectively, are connected by a 103.5-meter span. Under synchronous excitation, these piers tend to vibrate in phase, resulting in minimal relative displacement between them. However, when asynchronous ground motion is considered, the excitation reaches the piers at various times, leading to significant relative displacement that is not captured in the synchronous case. This increased relative movement can potentially cause unseating of girders from their supporting bearings, posing a risk to structural integrity. The relative displacement of P2 and P3 is shown in Figure 9 for asynchronous Elcentro excitation.

As observed from the analysis, asynchronous ground motion results in increased relative displacement between adjacent piers of the bridge. This differential movement arises due to the time lag and spatial

variation in seismic wave arrival, especially significant in long-span bridges or those with varying pier heights. Such increased relative displacement can introduce irregularities in the track alignment, potentially leading to misalignment or even damage to the continuous welded rail system. These irregularities pose a serious threat to the stability and safety of high-speed or trains with higher axle loads operating during or immediately after an earthquake. Therefore, considering asynchronous seismic effects is essential for the accurate assessment of track-structure interaction and the overall seismic safety of railway bridges.

5.3 Other significant observations

The input motion with wave passage effect and coherency losses can introduce significant variation in responses of some degree of freedom, which are otherwise observed to have negligible values under synchronous motion as input. A few superstructure nodes, such as node number 387 on span P3-P4 and node number 588 on span P1-P2, are considered for the study, which are rotational degree of freedom, i.e., torsion for the considered span. Figure 10 (a-b) clearly indicates that the torsion at those nodes is significantly higher for asynchronous and motion with wave passage effect than the similar values corresponding to the synchronous motion case. Similar observations were also made by Balamonica et al. [11] that the torsional degree of freedom is underestimated in analysis with synchronous input and may cause significant torsional stresses in the superstructure.

5.4 Effect on track curvature

The curvature of the deflected track under transverse seismic ground movement has been studied for the Elcentro EQ and Koyna EQ, for both synchronous and asynchronous motion. In Figure 9 (a-b), the curvature of the deflected track has been plotted along the length of the bridge at different time instances when the individual pier top deflection is maximum. Two such deflected track alignments corresponding to synchronous and asynchronous transverse ground movement, considering El-Centro and Koyna EQ, have been plotted and shown in Figure 10 (a-b) at the time instance when the deflection at the top of pier P3 is maximum. All the deflections are absolute, and the considered points have been joined by a spline to get the deflected shape of the track. The boundary condition to form the spline is, the angle of rotation of the track at the two abutment ends is zero, as the track beyond the abutments may be considered as aligned along the bridge axis. The curvature of the deflected shape of the track has been calculated along the length of the bridge from the spline coordinates.

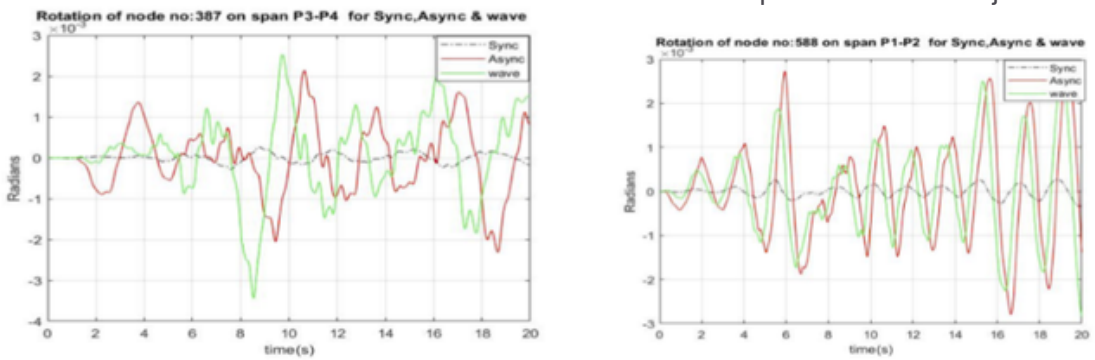

(a) At node 387 on span P3-P4 (b) At node 588 on span P1-P2

Fig. 10 Torsional Rotation Under El Centro Ground Motion

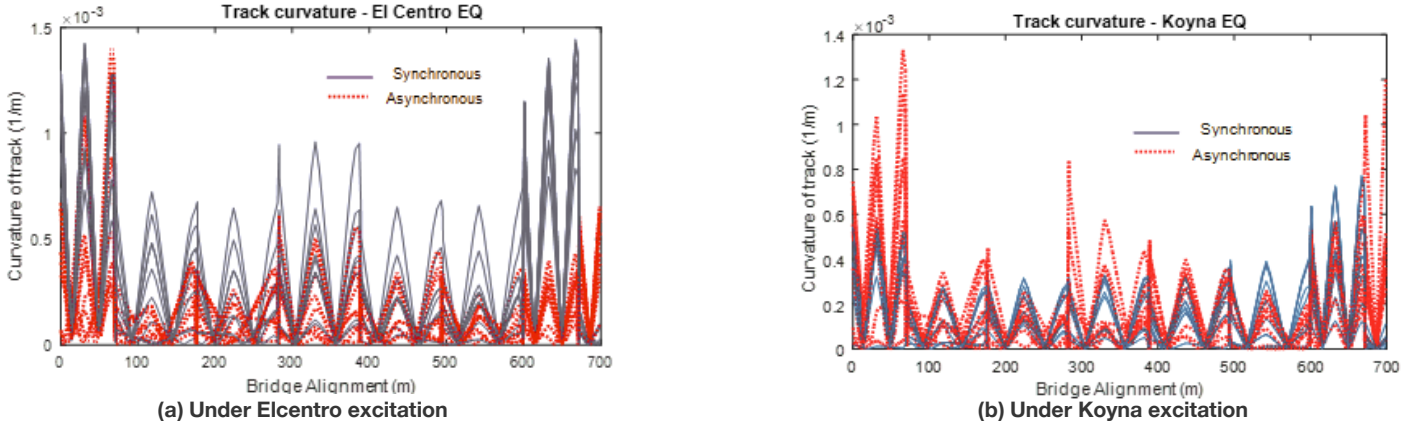

(a) Under Elcentro excitation **(b) Under Koyna excitation**

Fig. 11 Track Curvature for Synchronous and Asynchronous Ground Motion

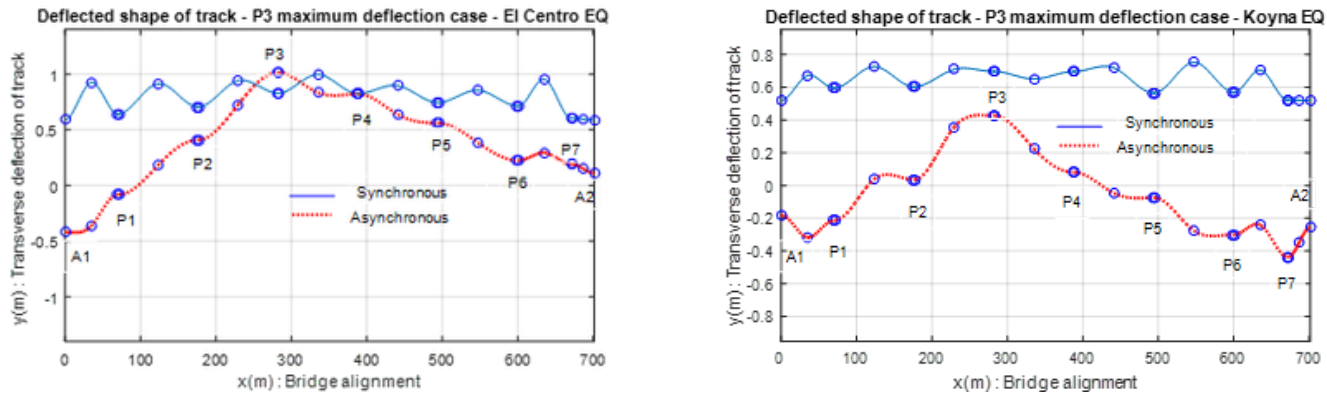

(a) Under Elcentro excitation **(b) Under Koyna excitation**

Fig. 12 Deflected shape of track for synchronous and asynchronous transverse ground motion considering Koyna EQ at the time instance when P3 pier top undergoes maximum deflection.

Similar curvature of the deflected shape of the track has been calculated for other time instances when the other pier top deflections are maximum, and all these curvature plots have been superimposed in Fig. 9(a) for Elcentro EQ and in Figure 9(b) for Koyna EQ. The safe velocity of the train during EQ varies with the curvature of the track. More is the curvature, the less will be the safe velocity. From Figure 9 (a) the track curvatures are less in the case of asynchronous ground motion compared to synchronous ground motion, considering the El-Centro EQ. Whereas in Figure 9(b), considering Koyna EQ the trend is reversed. This shows that track curvature for asynchronous ground motion may be higher or lower compared to the synchronous ground motion for different EQ time histories.

5.5 Derailment factors for the assessment of safety

The running safety or derailment of trains over bridges during seismic events remains a key focus of ongoing train bridge interaction research. The risk of derailment is assessed indirectly using force-based criteria and displacement criteria as discussed in this section.

Nadal [19] first proposed the well-known force-based derailment criterion, based on the equilibrium between lateral (Y) and vertical forces (Q) at the wheel flange during static flange-climb conditions. Nadal's formula for safety against derailment is given by:

$$\frac{Y}{Q} < \frac{tan\beta - \mu}{1 + \mu\, tan\beta}$$

where Y/Q is known as the derailment coefficient.

Although several authors have proposed modifications to Nadal's formula over the years, its simplicity has made it the most widely used formula in derailment investigations. Due to its conservative estimation of the Y / Q ratio, it is well-suited for ensuring safety. On the railways, a flange slope of 2.5:1 (tan β = 2.5 or β = 68°12') is typically used for the new wheel profile of carriages and wagons. Value of the coefficient of friction, μ depends on the geometry of the surfaces in contact, condition, and roughness of the surfaces, etc. On Indian Railways, μ in general is taken as 0.25. Thus, for β = 68° and μ = 0.25, Right Hand Side of the Nadal equation works out to 1.4. This is the threshold value. To allow for a certain margin or factor of safety, a limiting value of 1.0 for the ratio Y / Q has been laid down on the Indian Railways, as one of the criteria for assessment of rolling stock stability. ("out of white metal of the - Yumpu")

In addition to the force-based derailment criterion, displacement criteria based on the geometry of the wheel can also be used to check the stability of trains (Nishimura et al. [20], Tanabe et al. [21], Jin et al. [22]). The derailment is said to occur when the wheel lifts vertically to flange height (28.5 mm) and laterally slides from the initial regular position (63.5mm) as shown in Fig. 13.

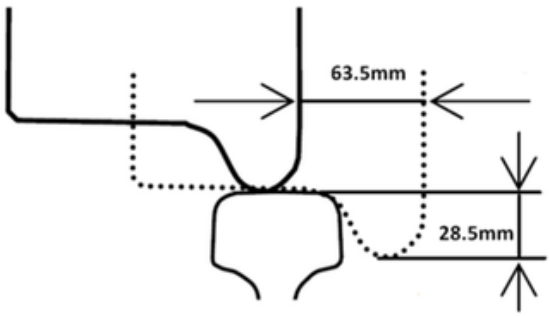

Fig. 13 Displacement Criteria for Derailment

From the analysis using train speed up to 120 kmph and corresponding to two different earthquakes, it has been found that the maximum value of the derailment coefficient is below 1.0. Similarly, both the vertical and lateral displacements are also below the limiting values. This trend has been observed considering both the synchronous and asynchronous ground motion.

6 Conclusions.

A long-span bridge with through type truss girder is considered for the analysis under simultaneous action of earthquake excitation and moving train. Finite element model of the bridge is made along with SSI using 1D nonlinear uncoupled springs. The bridge model is analysed using synchronous and asynchronous ground motions, and the responses of the bridge with a train moving at different speeds are studied. The responses of the Pier and deck are observed along with the relative displacement of adjacent piers. However, the derailment coefficient and displacement criteria revealed that the running train will remain safe for the input design spectrum compatible earthquake excitations considered.

The important conclusions are as follows:

- Increase in the displacement demand in piers and abutments is observed for the analysis with asynchronous input as compared to synchronous input-based analysis.
- Coherency losses in input motion may result in unseating of the superstructure due to larger relative displacement of adjacent piers.
- Active rotational degree of freedom that may lead to higher torsion in the superstructure, which is not found insignificant in the synchronous motion-based analysis.
- Effect of curvature in the track due to synchronous motion and asynchronous motion is case sensitive and depends on the characteristics of the ground motion itself.
- Bridge structure shows lesser displacement as well as acceleration response with a train on the bridge as compared to the case without train.

References

[1] S.Adanur, A.C.Altunisik, H.B. Başağa, K.Soyluk, A.A. Dumanoglu, “Wavepassage effect on the seismic response of suspension bridges considering local soil conditions," Int. J. Steel Struct., 17(2), 501–513, 2017.
[2] K. Konakli, A.D. Kiureghian,“Simulation of spatially varying ground motions including incoherence, wave-passage and differential site - response effects," Earthq. Eng. Struct. Dyn., 41, 495–513, 2012.
[3] J.L. Bogdanoff, J.E. Goldberg, A.J. Schiff, “The effect of ground transmission time on the response of long structures”, Bull. Seismol. Soc. America, 55, 627–640, 1965.
[4] A. Zerva, V. Zervas, “Spatial variation of seismic ground motions: An overview”, Applied Mechanics Reviews, 55, 271–296, 2002.
[5] D.I. Lavorato, I. Vanzi, C. Nuti, G. Monti. 2017. “Generation of non-synchronous earthquake signals”, Springer Series in Reliability Engineering, in: Paolo Gardoni (ed.), Risk and Reliability Analysis: Theory and Applications, pages 169-198, Springer, 2017.
[6] D. Basu , Rodda Gopala Krishnan, “Spatial variation and conditional simulation of seismic ground motion”, Bull Earthquake Eng., 16, 4399-4426, 2017.
[7] K. M. Berrah, “A modal combination rule for spatially varying", Earthq. Eng. Struct. Dyn., 22, 791–800, 1993.
[8] A.D.E.R.Kiureghian, A.Neuenhofer, “Response spectrum method for multisupport seismic excitations," Earthq. Eng. Struct. Dyn., 21, 713–740, 1992.

[[9] H. Mirzabozorg, M. Akbari, M.A. Hariri-Ardebili, “Nonlinear seismic response of a concrete arch dam to spatially varying earthquake ground motions," Asian J. Civil Eng. 14(6), 859–879, 2013.
[10] Y. H. Zhang, Q. S. Li, J. H. Lin,F. W. Williams, “Random vibration analysis of long-span structures subjected to spatially varying ground motions," Soil Dyn. Earthq. Eng., 29, 620–629, 2009.
[11] K. Balamonica., N. Gopalakrishnan, A. Ramamohan Rao,“Seismic Analysis of Structures Subjected to Spatially Varying Earthquake Using POD Vectors: Experimental and Analytical Studies”, Journal of Earthquake and Tsunami, 14(4), 2050017, 2020.
[12] Bo Li, Kaiming Bi, Nawawi Chouw, John W. Butterworth, Hong Hao, “Experimental investigation of spatially varying ground motions on bridge pounding," Earthq. Eng. Struct. Dyn. 41, 1959–1976, 2012.
[13] Nguyen, D. V., Kim, K. D., & Warnitchai, P. (2009). Simulation procedure for vehicle–substructure dynamic interactions and wheel movements using linearized wheel–rail interfaces. Finite Elements in Analysis and Design, 45(5), 341-356.
[14] Yang, Y. B., Yau, J. D., Yao, Z., & Wu, Y. S. (2004). Vehicle-bridge interaction dynamics: with applications to high-speed railways. World Scientific.
[15] American Petroleum Institute (API), “Recommended Practice for Planning, Designing and Constructing Fixed Offshore Platforms-Working Stress Design”, API Publishing Services: Washington, DC, USA, 2000.
[16] Computers and Structures, Inc. (CSI), “CSI Analysis Reference Manual for SAP2000”, Berkeley, CA, 2009.
[17] IS 1893, “Criteria for Earthquake Resistant Design of Structures- code of practice”, New Delhi, 2016.
[18] G. Fenton, E. H. A. Vanmarcke, “Conditioned simulation of local fields of earthquake ground motion”, Structural Safety, 10, 247–264, 1991.
[19] Nadal, M. J. (1896). Théorie de la stabilité des locomotives, Part 2: Mouvement de lacet. Annales des Mines, 10, 232
[20] Nishimura, K., Terumichi, Y., Morimura, T., & Sogabe, K. (2010). Analytical study on the safety of high-speed railway vehicle on excited tracks. Journal of System Design and Dynamics, 4(1), 211-225.
[21] Tanabe, M., Wakui, H., Sogabe, M., Matsumoto, N., & Tanabe, Y. (2011). An efficient numerical model for dynamic interaction of high-speed train and railway structure including post-derailment during an earthquake. In 8th International Conference on Structural Dynamics, EURODYN.
[22] Jin, Z., Pei, S., Li, X., Liu, H., & Qiang, S. (2016). Effect of vertical ground motion on earthquake-induced derailment of railway vehicles over simply supported bridges. Journal of Sound and Vibration, 383, 277-294.

Authors

Abhishek,
Post Graduate Student,
Civil Engng. Dept., IIT Guwahati, India

Prinza Priya Loying,
Research Scholar,
Civil Engng. Dept.,
IIT Guwahati, India

Sumantra Sengupta,
Research Scholar, Civil Engng. Dept., IIT Guwahati, India

Dr. Anjan Dutta,
Professor, Civil Engng. Dept., IIT Guwahati, India

Atmosphere Sky Bridge (Deya)

A Holistic Case study in Seismic Decoupling from Foundation to Sky

The Atmosphere Sky Bridge, officially named Deya ("cloud in Bengali"), represented a landmark achievement in integrated seismic design for mega structures in Kolkata, India. This is not a conventional bridge but a four-storey, 55,000 square foot "programmatic "sky bridge, housing an infinity pool, sports courts, and luxury amenities, suspended 100 meters above ground between two 150-meter-tall residential towers. Its entire immense weight and complex functionally are supported by just **four primary bearing** points. Completed in 2016, the project, designed by Arc Studio and engineered by Web structures, confronted the formidable triad of Kolkata's soft alluvial soil, high seismic zone (IS 1893 Zone III), and significant monsoon wind loads. Its elegant solution was a radical, system-wide philosophy of **controlled decoupling**, executed through a symbiotic design linking a deep foundation, dynamically independent towers, and an isolated skybridge via advanced **seismic isolation bearings**.

Kolkata's Eastern Metropolitan Bypass present a classic geotechnical challenge for high-rise construction: deep layers of soft, alluvial clay and slit with a high groundwater table, creating risks for bearing capacity, settlement, and potential liquefaction monumental skybridge, a conventional fixed base design would have led to prohibitive forces. The engineering philosophy, therefore, adopted a holistic Performance-Based Seismic Design (PBSD) approach that considered the soil-structure interaction, the tower dynamics, and the bridge response as one interconnected system.

> **"Rather than resisting nature with rigidity, the structure succeeds by intelligently yielding to it, allowing soil, towers, and bridge to move as a coordinated system."**

The core innovation was the strategic introduction of flexibility at two key interfaces: between the ground and the towers, and between the towers and the bridge. The deep pile foundation manages geotechnical uncertainty, while the seismic isolation bearings on the 30th floor create a kinematic decoupling. This seismic horizontal force from the bridge to the towers by approximately 50% effectively lowers the demand on every structural element below from the outriggers and shear walls down to the foundation piles. This cascading reduction in force is the cornerstone of the project's efficiency and resilience.

The aspiration to create a “floating cloud” directly drove the structural solution. The Deya bridge is a masterwork of steel engineering, a free-form space truss weighing 2,500 tons comprising over 1,500 sections connected via a precise MERO PLUS node system. Its form is an assembly that rests upon just four points, where the seismic isolation bearings are located.

The supporting towers are 39-story reinforced concrete structures, employing robust core walls and outrigger systems designed for inherent stiffness. Crucially, their design had to account for the integration enabled by the bearings. The architectural expression of a lightweight, separate cloud is thus a direct result of this deliberate structural separation, achieved not by visual trickery but by profound seismic engineering.

Diagrid and Trusses: Integration of primary and secondary trusses forming a lightweight diagrid mesh for robustness and flexibility against Kolkata’s wind and seismic forces.

> **“The diagrid does not merely support the form; it becomes the form, distributing forces with both strength and elegance.”**

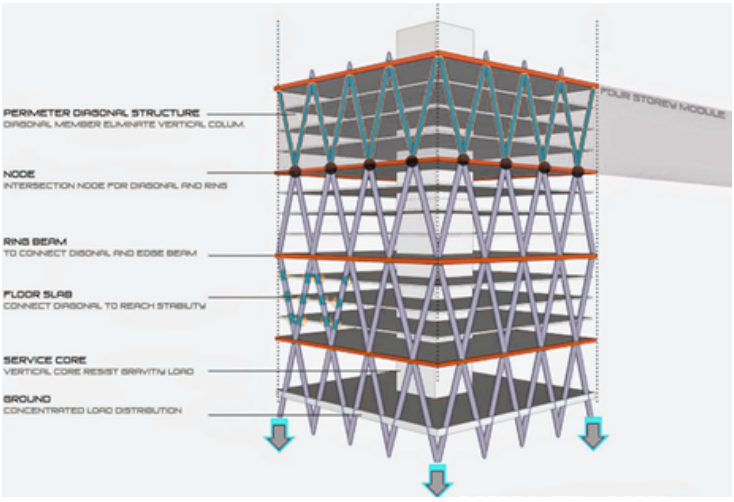

Fig. 1 Diagrid system diagram

The Foundation: Anchoring Resilience in Soft Soil

The stability of the entire system originates from its deep foundation. To anchor the 150-meter towers and resist the combined overturning moments from wind, seismicity, and the bridge, a high-capacity deep foundation system was employed.

Pile Foundation:

Large diameter bored cast-in-situ piles (often existing 30-40 meters in depth in Kolkata); this system penetrates the soft alluvial strata to derive load capacity from deeper, more stable bearing layers. This mitigates risks of differential settlements and liquefaction-induced failure.

The foundation must support not only the gravity loads of the towers but also the significant additional vertical and lateral loads transferred from the Sky bridge. The success of the EradiQuake bearings in reducing lateral seismic force by 50% directly lessens the shear and the overturning demands on these piles, optimizing their design. Furthermore, the foundation is engineered to resist tensile uplift forces generated during extreme wind events on the slender tower profiles.

The four **EradiQuake Seismic isolation bearings,** each weighing 17,128kg, are used for decoupling. Positioned at the bridge supports on the 30th floor, they act as sophisticated mechanical filters.

Each bearing is designed to support a massive **vertical load of 30000 kN.** These bearings include wind fuses to prevent unwanted activation under lateral wind loads and accommodate a longitudinal seismic displacement of 200 mm and a lateral movement of 250 mm. Their design includes a **Mass Energy Regulator (MER)** for damping and a unique wind restraint mechanism. **PTFE/stainless steel sliding** interfaces into potential **frictional damping**.

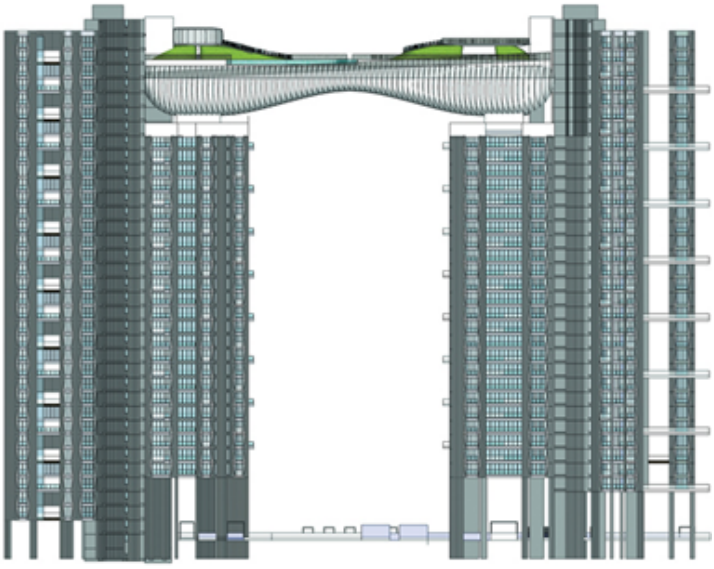

> **“The bridge’s apparent weightlessness is the outcome of deliberate structural intelligence, where diagrids, trusses, and isolation systems transform immense mass into controlled lightness.”**

This allows the structure to resist frequent, high-intensity wind loads (1,500 kN) as a fixed connection while smoothly transitioning to an isolated state during a seismic event, managing a reduced force of approximately 1,800 kN. Bearings were installed with **anchoring plates and pressure grouting** to ensure precise levelling and stability.

By lengthening the effective period of the bridge and adding damping, the bearings dramatically reduce the acceleration and force transmitted to the bridge's deck. This protection of the expensive architectural content is coupled with the foundational benefit of lowering the base shear and moment that the towers and their deep piles must withstand.

References

1. RJ Watson, Inc. (2014). Project Technical Specifications & 2024 Inspection Report: EradiQuake Bearings for Atmosphere Sky Bridge.
2. Web Structures & M.N. Consultants. (2016). Integrated Structural and Foundation Design Report, Atmosphere Project.
3. Bureau of Indian Standards. (2002). IS 1893 (Part 1): Criteria for Earthquake Resistant Design of Structures.
4. Bureau of Indian Standards. (2007). *IS 2911 (Part 1/Sec 2): Design and Construction of Pile Foundations*.
5. Naeim, F., & Kelly, J. M. (1999). Design of Seismic Isolated Structures: From Theory to Practice. John Wiley & Sons.

Join the Online Quiz Competition on

Seismic Safety and Strengthening of Structures

Start : 15th April 2026
End : 30th April 2026

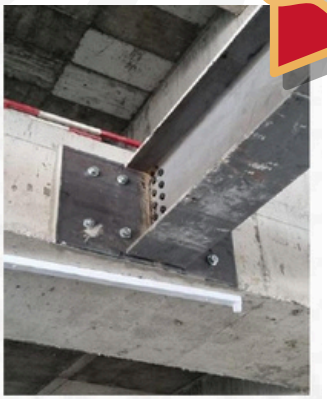

to Register

2nd January
Mexico

4th January
India

6th January
Japan

19th January
Pakistan

5th February
Indonesia

27th February
Bangladesh

13th March
Turkey

Rescue workers search for survivors in Naypyitaw. (AP: Aung Shine Oo)

Tracking Recent 2026 Earthquakes

Mexico

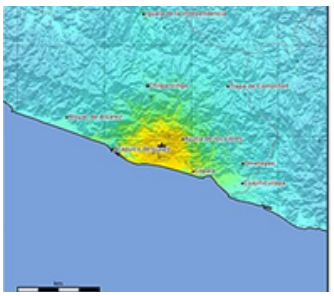

Date: 2nd January, 2026
Magnitude: 6.5
Epicenter: near San Marcos, 18 km depth
Impacts: 2 dead, 24 injured

India

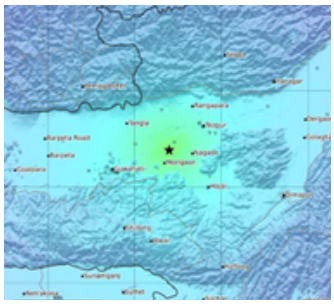

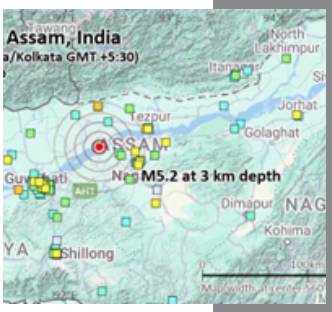

Date: 4th January, 2026
Magnitude: 5.2
Epicenter: located in Morigaon/Dhing- 13 km depth
Impacts: 3 injured

Japan

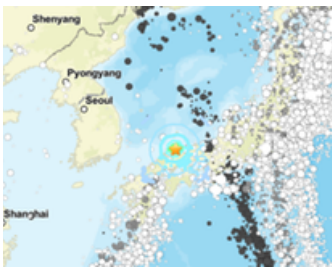

Date: 6th January, 2026
Magnitude: 5.7
Epicenter: Matsue - 18 km depth
Impacts: 15 injured

Pakistan

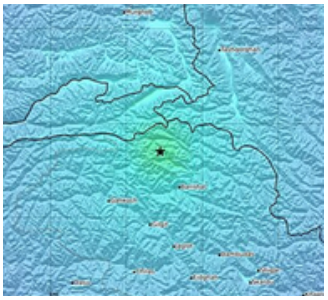

Date: 19th January, 2026
Magnitude: 5.6
Epicenter: 47 km NNW of Barishal- 23km depth
Impacts: 2 dead, 5 injured

Indonesia

Date: 5th February, 2026
Magnitude: 5.8
Epicenter: 94 km SW of Trenggalek - 40 km depth
Impacts: 1 dead, 47 injured

Bangladesh

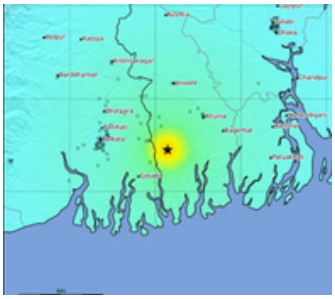

Date: 27th February, 2026
Magnitude: 5.0
Epicenter: 23 km SSE of Satkhira – 10 km depth
Impacts: 3 injured

Turkey

Date: 13th March, 2026
Magnitude: 5.3
Epicenter: 16 km east of Erbaa – 10 km depth
Impacts: Some people injured or hospitalized and minor damage in the Tokat area

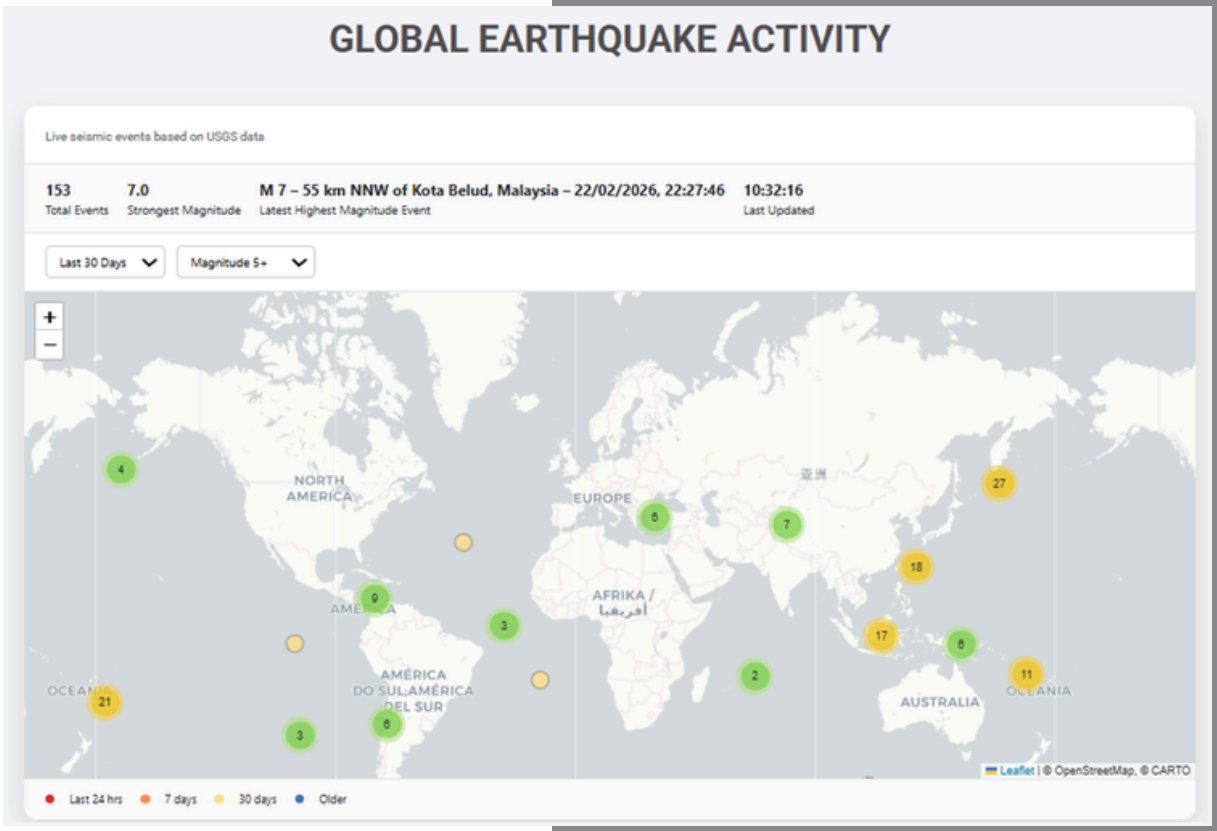

The Global Earthquake Map is also LIVE on the **Seismic Academy website**:
The map shows live tracking of earthquakes along with the highest magnitude earthquake details with epicentre.

Test your Seismic Engineering Acumen

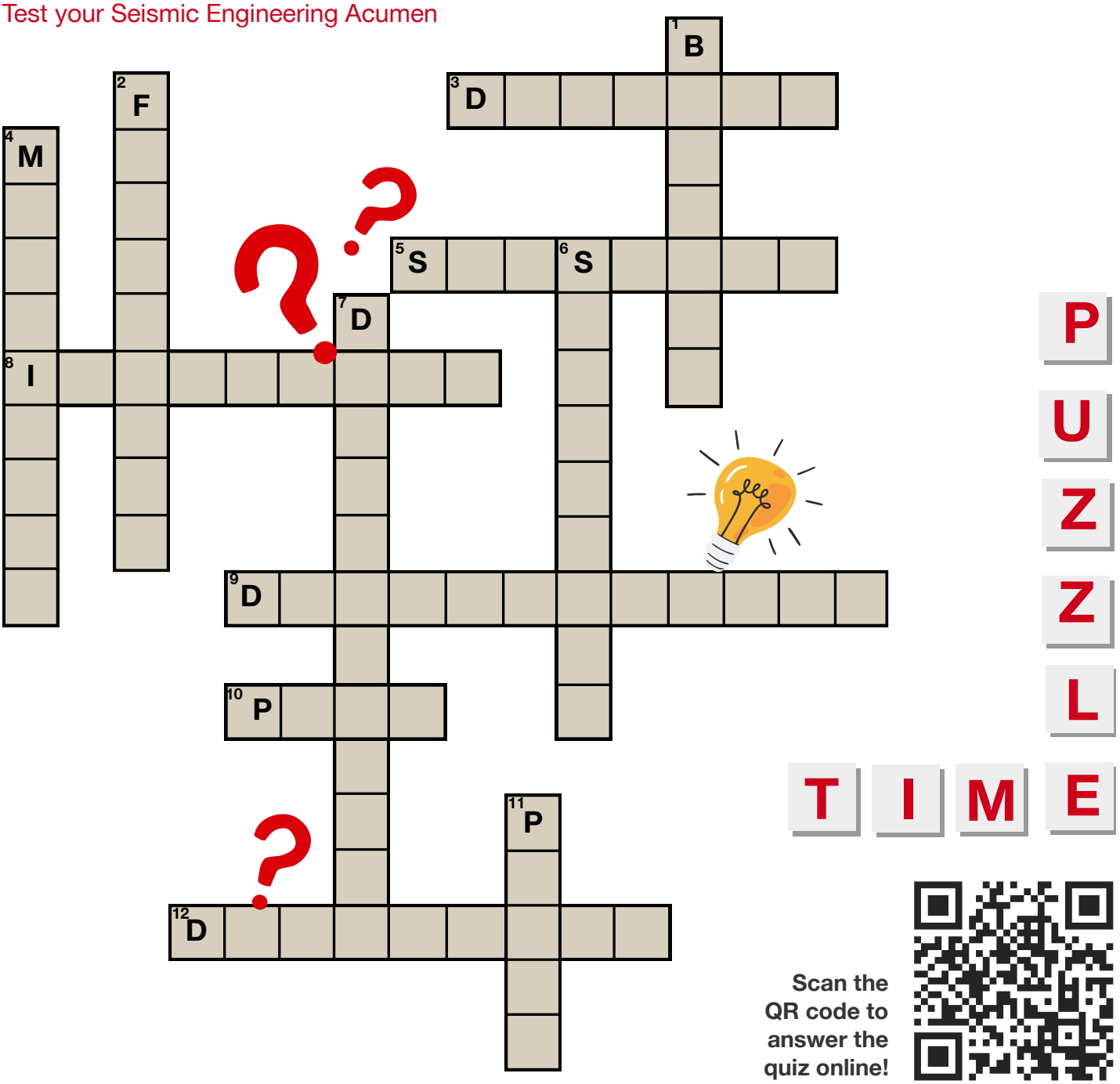

Scan the QR code to answer the quiz online!

DOWN

1. Structural system used in steel frames to resist lateral seismic forces.
2. Vertical distance between the highest level of contained water and the top of the container, such as a dam crest or tank, provided to prevent overtopping during an earthquake
4. Numerical measure of the energy released during an earthquake, for example the 7.6 Kashmir event mentioned in the journal.
6. The suspended structure connecting two towers in the Atmosphere project in Kolkata.
7. The physical shift, offset, or movement of the ground or a structure from its original position due to earthquake forces
11. Deep foundation elements used in soft soils to support tall structures like the Atmosphere towers.

ACROSS

3. Structural mesh system used in the Atmosphere Sky Bridge to distribute loads efficiently
5. Low-frequency, and large-amplitude movement of a liquid's free surface within a container (such as a water tank, oil reservoir, or fuel tank) caused by earthquake-induced ground shaking
8. Seismic design strategy that decouples a structure from ground motion using bearings.
9. Traditional Kashmiri earthquake resistant construction system forming patchwork walls.
10. A vertical, intermediate substructure that supports the span of a bridge, transferring vertical and horizontal loads to the foundation
12. Structural property that allows controlled deformation and energy dissipation during earthquakes.

SEISMIC ACADEMY

Stay tuned for insights on best seismic practices

Click to view the YouTube channel

Scan the QR code or Click to access the website